

# UC Berkeley

## UC Berkeley Previously Published Works

### Title

Constraints on the formation and diagenesis of phosphorites using carbonate clumped isotopes

### Permalink

<https://escholarship.org/uc/item/5dm6b94h>

### Authors

Stolper, Daniel A  
Eiler, John M

### Publication Date

2016-05-01

### DOI

10.1016/j.gca.2016.02.030

Peer reviewed

# Constraints on the formation and diagenesis of phosphorites using carbonate clumped isotopes

Author links open overlay panel [Daniel A. Stolper<sup>a1</sup>](#) [John M. Eiler<sup>a</sup>](#)  
Show more

<https://doi.org/10.1016/j.gca.2016.02.030> [Get rights and content](#)

## Abstract

The [isotopic composition](#) of apatites from sedimentary [phosphorite](#) deposits has been used previously to reconstruct ancient conditions on the surface of the Earth. However, questions remain as to whether these minerals retain their original isotopic composition or are modified during burial and [lithification](#). To better understand how apatites in phosphorites form and are diagenetically modified, we present new isotopic measurements of  $\delta^{18}\text{O}$  values and clumped-isotope-based ( $\Delta_{47}$ ) temperatures of [carbonate groups](#) in apatites from phosphorites from the past 265 million years. We compare these measurements to previously measured  $\delta^{18}\text{O}$  values of [phosphate groups](#) from the same apatites. These results indicate that the isotopic composition of many of the apatites do not record environmental conditions during formation but instead diagenetic conditions. To understand these results, we construct a model that describes the consequences of diagenetic modification of phosphorites as functions of the environmental conditions (i.e., temperature and  $\delta^{18}\text{O}$  values of the fluids) during initial precipitation and subsequent [diagenesis](#). This model captures the basic features of the dataset and indicates that clumped-isotope-based temperatures provide additional quantitative constraints on both the formational environment of the apatites and subsequent diagenetic modification. Importantly, the combination of the model with the data indicates that the  $\delta^{18}\text{O}$  values and clumped-isotope temperatures recorded by phosphorites do not record either formation or diagenetic temperatures, but rather represent an integrated history that includes both the formation and diagenetic modification of the apatites.

- [Previous article](#)
- [Next article](#)

## 1. Introduction

[Paleotemperature](#) reconstructions are a key area of research in [Earth science](#). Although many geochemical tools exist to make these reconstructions, an early and still widely used technique is based on [oxygen-isotope](#) analyses of carbonate-bearing minerals like [calcite](#) and [aragonite](#) ([McCrea, 1950](#), [Epstein et al., 1953](#)). Oxygen-isotope-based

reconstructions (represented using  $\delta$  notation<sup>2</sup>) of mineral formation temperatures require independent knowledge of the [isotopic composition](#) the formational fluids. Additionally, samples cannot have been isotopically altered after deposition. Problematically, constraints on the isotopic composition of the original formational fluids as well as the isotopic integrity of carbonate-bearing minerals over [geological time](#) are old, persistent, controversial, and unresolved issues (e.g., [Degens and Epstein, 1962](#), [Killingley, 1983](#), [Muehlenbachs, 1986](#), [Veizer et al., 1986](#), [Veizer et al., 1997](#), [Veizer et al., 1999](#), [Schrag et al., 1992](#), [Schrag et al., 1995](#), [Land, 1995](#), [Lécuyer and Allemand, 1999](#), [Kasting et al., 2006](#), [Jaffrés et al., 2007](#), [Came et al., 2007](#), [Trotter et al., 2008](#), [Finnegan et al., 2011](#), [Veizer and Prokoph, 2015](#)).

With foresight on these potential concerns, [Urey et al. \(1951\)](#) suggested that the oxygen-isotope composition of [apatite](#), which is a function temperature ([Urey, 1947](#), [Longinelli and Nuti, 1973](#), [Kolodny et al., 1983](#)), could be used to complement and independently test calcite- and aragonite-based  $\delta^{18}\text{O}$  temperature reconstructions. Furthermore,  $\text{PO}_4^{3-}$  groups in apatite have been suggested to be more resistant to post-depositional isotopic exchange than  $\text{CO}_3^{2-}$  groups in calcite and aragonite ([Kolodny et al., 1983](#), [Shemesh et al., 1983](#), [Longinelli et al., 2003](#)). Thus, they are sometimes preferred for isotope-based temperature reconstructions

Apatites are also of interest for isotopic studies as they can contain structural  $\text{PO}_4^{3-}$  and  $\text{CO}_3^{2-}$  groups, both of which can be independently analyzed for  $\delta^{18}\text{O}$  ([Tudge, 1960](#), [Longinelli and Nuti, 1968](#), [Longinelli and Nuti, 1973](#), [Kolodny and Kaplan, 1970](#), [Shemesh et al., 1983](#), [Shemesh et al., 1988](#)). Such measurements are denoted as  $\delta^{18}\text{OPO4}$  and  $\delta^{18}\text{OCO3}$  respectively. When combined, these allow for the calculation of formation temperatures that are independent of the isotopic composition of the water in which the apatite formed ([Shemesh et al., 1983](#)).

Apatite from phosphatic brachiopod shells (e.g., [Lécuyer et al., 1996](#), [Lécuyer et al., 1998](#), [Wenzel et al., 2000](#)), teeth and bones (e.g., [Kolodny et al., 1983](#), [Longinelli, 1984](#), [Luz et al., 1984a](#), [Kolodny and Luz, 1991](#), [Ayliffe et al., 1994](#), [Sharp et al., 2000](#), [Kohn and Cerling, 2002](#), [Eagle et al., 2011](#)), conodonts (e.g., [Luz et al., 1984b](#), [Wenzel et al., 2000](#), [Trotter et al., 2008](#), [Sun et al., 2012](#)), and authigenic [phosphorite](#) deposits ([Longinelli and Nuti, 1968](#), [Shemesh et al., 1983](#), [Shemesh et al., 1988](#), [Ayliffe et al., 1992](#), [Hiatt and Budd, 2001](#), [Jaisi and Blake, 2010](#)) have all been used for paleotemperature reconstructions. Phosphorites, which are the focus of this study, were some of the earliest apatite samples used for  $\delta^{18}\text{OPO4}$ -based reconstructions of ancient surface conditions ([Longinelli and Nuti, 1968](#), [Shemesh et al., 1983](#)). These studies showed that the  $\delta^{18}\text{OPO4}$  values

of [Phanerozoic](#) phosphorite apatites decrease with increasing depositional age, mirroring a similar decline in  $\delta^{18}\text{O}$  values of carbonates. Due to the perceived resistance of  $\text{PO}_4^{3-}$  groups to post-depositional isotopic modification, [Shemesh et al. \(1983\)](#) argued that the signal of decreasing  $\delta^{18}\text{OPO}_4$  reflected changing environmental conditions. This requires that either the ocean tens to hundreds of millions of years ago was significantly (e.g.,  $\sim 10+$  °C) warmer than today, or that the  $\delta^{18}\text{O}$  value of the ocean was lower than today (by multiple per mil), or some combination of the two effects.

However, after these initial studies, it was recognized that apatite  $\text{PO}_4^{3-}$  oxygen is not impervious to isotope exchange after mineral formation ([Shemesh et al., 1988](#), [McArthur and Herczeg, 1990](#), [Kastner et al., 1990](#), [Ayliffe et al., 1994](#), [Kolodny et al., 1996](#), [Sharp et al., 2000](#), [Wenzel et al., 2000](#), [Zazzo et al., 2004](#)). For example, microbially mediated reactions can catalyze the exchange of oxygen isotopes between phosphate and water ([Blake et al., 1997](#), [Zazzo et al., 2004](#)). Thus, a critical question for all paleoclimate-driven studies of apatites that employ oxygen isotopes is do measured  $\delta^{18}\text{O}$  values reflect original mineral formation temperatures? Or, alternatively, do they reflect some other aspect of the sample's diagenetic and subsequent geological history? This is a particularly troublesome question for studies of phosphorites because there are no agreed upon geochemical or petrographic criteria that can be used to establish whether or not a given sample has been diagenetically altered ([Shemesh et al., 1983](#), [Shemesh et al., 1988](#), [Shemesh, 1990](#)).

In order to contribute to the understanding of how and under what conditions sedimentary apatites form and are modified during burial and [lithification](#), we made 'clumped-isotope' measurements of [carbonate groups](#) in phosphorite apatite with depositional ages from near modern to 265 million years old and compared them to measured  $\delta^{18}\text{OCO}_3$  and  $\delta^{18}\text{OPO}_4$  values on the same samples. Carbonate clumped-isotope measurements quantify the amount of multiply isotopically substituted (clumped) carbonate groups that generate mass-47  $\text{CO}_2$  molecules ( $^{13}\text{C}^{16}\text{O}^{18}\text{O}$ ,  $^{12}\text{C}^{17}\text{O}^{18}\text{O}$ ,  $^{13}\text{C}^{17}\text{O}_2$ ) during [acid digestion](#) ([Ghosh et al., 2006](#)). At isotopic equilibrium, clumped isotopologues are enriched compared to a [random distribution](#) of isotopes amongst all isotopologues. Importantly, the size of the enrichment is a unique function of temperature and thus can be used for paleotemperature reconstructions (e.g., [Wang et al., 2004](#), [Schauble et al., 2006](#), [Eiler, 2007](#), [Eiler, 2011](#), [Eiler, 2013](#), [Dennis and Schrag, 2010](#), [Zaarur et al., 2013](#), [Defliese et al., 2015](#), [Kluge et al., 2015](#)). Clumped-isotope abundances of carbonates are quantified with the symbol  $\Delta_{47}^3$ , which is a monotonic function of mineral formation temperature (e.g., [Ghosh et al., 2006](#), [Dennis and Schrag, 2010](#), [Zaarur et al., 2013](#), [Defliese et al., 2015](#), [Kluge et al., 2015](#)).

Because clumped-isotope temperatures are independent of the isotopic composition of the waters from which minerals form, such measurements can provide new constraints on a sample's chemical and physical formational conditions and geological history. This includes allowing for the calculation of the isotopic composition of the [formation waters](#) (e.g., [Came et al., 2007](#), [Finnegan et al., 2011](#), [Ferry et al., 2011](#), [Petersen and Schrag, 2015](#)). Here we explore the additional constraints clumped-isotope temperatures can provide on the conditions of phosphorite formation and modification when combined with  $\delta^{18}\text{O}$  measurements of both structural phosphate and carbonate groups. Because both the temperature based on the  $\delta^{18}\text{OPO}_4$ — $\delta^{18}\text{OCO}_3$  [fractionation](#) and that based on the clumped-isotope technique can be measured within a single phase, one mineral can yield two independent constraints on a sample's formation temperature. These temperatures should reflect either the conditions under which phosphorites formed or were later modified. For example, if the temperatures disagree, it would likely indicate either non-equilibrium precipitation or [diagenesis](#) post formation. Such a strategy was used by [Eagle et al. \(2011\)](#) to distinguish pristine fossil samples of [dinosaur](#) teeth from those diagenetically altered. Here, we provide a framework for the quantitative interpretation of the meaning of  $\delta^{18}\text{OPO}_4$  —  $\delta^{18}\text{OCO}_3$  fractionations vs. clumped-isotope measurements, and a critical examination into the insights such a 'dual-thermometer' approach can provide. Specifically, we demonstrate that measurements of clumped-isotope temperatures in combination with  $\delta^{18}\text{OPO}_4$  and  $\delta^{18}\text{OCO}_3$  measurements allow for both the identification of samples that have been diagenetically modified as well as the 'style' of that diagenesis: e.g., open, water-buffered vs. closed-system diagenesis and the extent of diagenetic overprinting. We show that many samples yield clumped-isotope temperatures that are distinct from the temperatures inferred solely using  $\delta^{18}\text{OPO}_4$  vs.  $\delta^{18}\text{OCO}_3$  values. We suggest that this disagreement is caused by different oxygen-isotope-exchange rates of  $\text{PO}_4^{3-}$  and  $\text{CO}_3^{2-}$  groups with water during diagenesis. Such differing rates would allow a mineral, during diagenesis, to yield phosphate and carbonate groups out of equilibrium with each other.

To explore this hypothesis quantitatively, we develop a model to describe the water-buffered diagenesis of  $\delta^{18}\text{OPO}_4$ ,  $\delta^{18}\text{OCO}_3$ , and  $\Delta_{47}$  values in apatite and fit the model to the measured data. This model yields the insight that inferred clumped-isotope-based temperatures of the diagenetically modified apatites do not represent the temperature at which diagenesis took place, as is sometimes assumed in clumped-isotope studies. Instead the clumped-isotope temperatures reflect the integrated history of the mineral from formation through diagenesis. This inference is then placed in the context of a

qualitative model of apatite growth and modification in phosphorites, informed by commonly observed fabrics of such rocks. We note that the data and models presented here were originally presented in a graduate Ph.D. thesis ([Stolper, 2014](#)). Additionally, a recent study reported three measurements of clumped-isotope temperatures of apatites from the Monterey Formation phosphorite ([Bradbury et al., 2015](#)), but did not include  $\delta^{18}\text{OPO}_4$  measurements. We comment on these results in the context of the samples measured in this study below.

## 2. Materials and methods

### 2.1. Materials

[Phosphorite](#) samples measured in this study are listed in [Table 1](#) and are the same as those used in [Shemesh et al. \(1983\)](#) and [Shemesh et al. \(1988\)](#), except for NBS 120C. All  $\delta^{18}\text{OPO}_4$  values are from [Shemesh et al. \(1988\)](#) and were measured as  $\text{BiPO}_4$ , except NBS 120C, which was analyzed as  $\text{Ag}_3\text{PO}_4$  ([Pucéat et al., 2010](#), [Lécuyer et al., 2013](#)). Because there is an apparent offset between  $\delta^{18}\text{OPO}_4$  values measured using  $\text{BiPO}_4$  vs.  $\text{Ag}_3\text{PO}_4$  ([Pucéat et al., 2010](#), [Lécuyer et al., 2013](#)), we converted NBS 120C to the  $\text{BiPO}_4$ -method 'reference frame'. We did this by assuming a  $\delta^{18}\text{OPO}_4$  value of 20‰ for NBS 120B when measured using the  $\text{BiPO}_4$  method ([Pucéat et al., 2010](#), [Lécuyer et al., 2013](#)) and an offset of 0.3‰ between NBS 120B and 120C, which was found using an  $\text{Ag}_3\text{PO}_4$  method ([Lécuyer et al., 2013](#)). This results in a  $\delta^{18}\text{O}$  value of 20.3‰ for NBS 120C in the  $\text{BiPO}_4$  method reference frame.

Table 1. Age, location, and bulk [isotopic compositions](#) of all samples measured.

Sample	Location	Age (ma)	$\delta^{13}\text{C}$ (‰) (this study) <sup>a</sup>	$\pm^b$	$\delta^{18}\text{OCO}_3$ (‰) (this study) <sup>c</sup>	$\pm^b$	$\delta^{13}\text{CCO}_3$ (‰) ( <a href="#">Shemesh et al., 1988</a> ) <sup>a</sup>	$\delta^{18}\text{OCO}_3$ (‰) ( <a href="#">Shemesh et al., 1988</a> ) <sup>c</sup>	$\delta^{18}\text{OPO}_4$ (‰) ( <a href="#">Shemesh et al., 1988</a> ) <sup>c,d</sup>
ASP 3	Phosphoria, USA <sup>f</sup>	265	-3.30	0.0	17.59	0.0	-3.5	16.8	15.8
				2		7			
ASP 4	Monterey, Mexico <sup>f</sup>	30	-6.79	0.0	25.89	0.0	-6.8	24	19.1
				1		8			
ASP 9	Rassaif, Israel <sup>f</sup>	75	-8.69	0.0	24.43	0.0	-9.9	21.8	19
				1		4			
ASP 15	G. Rechavam, Israel <sup>f</sup>	75	-7.27	0.0	23.54	0.1	-6.8	22.8	17.3
				4		4			
ASP 22	Off-Shore, Namibia <sup>g</sup>	1–5 <sup>h</sup>	-1.90	0.0	35.05	0.2	-1.9	32.7	23.4
				3		1			

Sample	Location	Age (ma)	$\delta^{13}\text{C}$ (‰) (this study) <sup>a</sup>	$\pm^b$	$\delta^{18}\text{OCO}_3$ (‰) (this study) <sup>c</sup>	$\pm^b$	$\delta^{13}\text{CCO}_3$ (‰) (Shemesh et al., 1988) <sup>a</sup>	$\delta^{18}\text{OCO}_3$ (‰) (Shemesh et al., 1988) <sup>c</sup>	$\delta^{18}\text{OPO}_4$ (‰) (Shemesh et al., 1988) <sup>c,d</sup>
ASP 28	Sechura, Peru <sup>f</sup>	14	-5.22	0.0	31.36	0.0	-5.1	30.4	22.3
ASP 46	Quseir, Egypt <sup>f</sup>	75	-5.70	0.0	21.13	0.1	-6.3	21.3	17.7
ASP 49	Monterey, Baja <sup>f</sup>	30	-6.88	0.0	25.69	0.0	-6.9	25.4	19
ASP 78	Blake Plateau <sup>g</sup>	26	-0.52	0.0	31.69	0.1	-1.1	31.1	23
ASP 84	Oron, Israel <sup>f</sup>	75	-9.52	0.0	25.50	0.1	-10.5	26.5	20.2
ASP 105	Central Florida, USA <sup>f</sup>	3.4	-5.45	0.0	29.03	0.0	-5.7	28.2	20.4
NBS 120C			-6.29	0.0	29.40	0.0	-	-	20.3
ASP 6 <sup>e</sup>	Arad, Israel <sup>f</sup>	75	-8.34	0.0	24.59	0.1	-8.3	22.5	18.6
ASP 12 <sup>e</sup>	Bir Zafra, Egypt <sup>f</sup>	75	-6.90	0.0	21.56	0.2	-5.1	21.5	16.2

a

Referenced to the VPDB scale.

b

1 standard error.

c

Referenced to VSMOW.

d

Measured on  $\text{BiPO}_4$  except for NBS 120c (measured as  $\text{Ag}_3\text{PO}_4$ ), which has been converted to the  $\text{BiPO}_4$  reference frame. See Section 2.1.

e

Produced larger quantities of  $\text{CO}_2$  than other experiments and thus are excluded from all discussion in case of contamination by exogenous carbonate phases not removed during acid washing.

f

Outcrop sample.

g

Dredged from the seafloor.

h

Reported in [Shemesh et al. \(1988\)](#) as <10,000 years old. However, the sample is described in [Shemesh \(1990\)](#) as a glauconized pelletal phosphorite. Pelletal phosphorites from off-shore Namibia were dated in [Thomson et al. \(1984\)](#) as older than 700,000 years using  $^{230}\text{Th}/^{234}\text{U}$ , dating. [McArthur et al. \(1990\)](#) dated Namibian pelletal phosphorites as being between 1 and 5 million years old using strontium isotopes. Such ages are consistent with the facies model of [Bremner and Rogers \(1990\)](#) and are adopted here.

## 2.2. Sample preparation

All measured phosphorite samples were previously powdered before delivery to the Caltech laboratories. [Grain sizes](#) were not measured. Each sample was first treated with 3%  $\text{H}_2\text{O}_2$  at room temperature for 4 h to remove any [organic contaminants](#) and then washed 3 times in deionized (DI) water. Samples were subsequently treated with buffered [acetic acid](#) (0.1 M, pH = 4.5) for 48 h to remove exogenous carbonate minerals (i.e., carbonate not dissolved in the phosphate lattice), washed 3 times in deionized water, then dried overnight in a 70 °C oven. This procedure follows those described in [Eagle et al. \(2010\)](#). We note that based on experiments with apatites in the lab, heating samples overnight at 70 °C is unlikely to alter measured clumped-isotope temperatures. For example, holding samples at ~400 °C for a week does not, within analytical error, alter clumped-isotope compositions of igneous apatites ([Stolper and Eiler, 2015](#)).

## 2.3. Isotopic measurements

Measurements of  $\delta^{13}\text{CCO}_3$  (the  $\delta^{13}\text{C}$  value of [carbonate groups](#) dissolved in apatite) and  $\delta^{18}\text{OCO}_3$  ([Table 1](#)) and  $\Delta_{47}$  ([Table 2](#)) values of carbonate groups dissolved in [apatite](#) were made on  $\text{CO}_2$  evolved from the [acid digestion](#) of phosphates at Caltech. Samples were digested for 20 min in a 90 °C stirred acid bath with 104% [phosphoric acid](#) on two nearly identical automated extraction lines as described in [Passey et al. \(2010\)](#) and [Eagle et al. \(2010\)](#). The [isotopic composition](#) of  $\text{CO}_2$  was measured on two separate [mass spectrometers](#) following procedures outlined in [Eiler and Schauble \(2004\)](#) and [Huntington et al. \(2009\)](#). Note that some samples, but not all, were measured using both extraction lines and mass spectrometers.  $\delta^{13}\text{C}$  and  $\delta^{18}\text{O}$  values of



samples were determined through comparison to a gas with a known isotopic composition using an ion-correction algorithm in the Isodat software program (Huntington et al., 2009) and standardized to the VPDB scale for [carbon-isotope](#) measurements and VSMOW for [oxygen-isotope](#) measurements. Carbonate  $\delta^{18}\text{O}$  values were calculated from the  $\text{CO}_2$  values assuming that the isotopic [fractionation](#) factor ( $^{18}\text{R}_{\text{CaCO}_3}/^{18}\text{R}_{\text{CO}_2}$ ) for phosphoric acid digestion at 90 °C is 1.00821 (Swart et al., 1991). We thus assume that carbonate dissolved in apatite has the same oxygen-isotope acid-digestion fractionation factor as [calcite](#). We note that different acid-digestion fractionation factors have been suggested for [hydroxyapatite](#) from fossil material (Passey et al., 2007) as compared to those used for calcite. Using these apatite-specific fractionation factors would shift our measured  $\delta^{18}\text{O}$  values of carbonate groups in apatite to values  $\sim 0.5\text{‰}$  to  $1\text{‰}$  lower than reported here. However, we do not use these alternative fractionation factors as the differences they introduce are not significant to the study here nor have they been studied for [fluorapatites](#) (the mineralogical form of apatites in phosphorites).

Table 2.  $\Delta_{47}$  values and calculated clumped-isotope-based temperatures for all samples measured.

Sample	$n^a$	$\Delta_{47,\text{ARF}}$ (‰) <sup>b</sup>	$\pm^c$	$\Delta_{48}$	$\pm^c$	$T_{\text{ARF}}$ (°C) <sup>d</sup>	$\pm^c$
ASP 3	4	0.613	0.010	0.0	0.2	47	2
ASP 4	6	0.685	0.009	0.5	0.2	30	2
ASP 9	4	0.659	0.007	0.3	0.0	36	2
ASP 15	5	0.654	0.012	0.6	0.5	37	3
ASP 22	7	0.724	0.011	0.2	0.1	22	2
ASP 28	4	0.678	0.007	0.5	0.1	32	2
ASP 46	5	0.601	0.011	0.3	0.2	51	3
ASP 49	6	0.665	0.011	0.3	0.1	35	2
ASP 78	4	0.696	0.009	0.5	0.1	28	2
ASP 84	4	0.658	0.010	0.5	0.2	36	2
ASP 105	5	0.663	0.008	0.5	0.1	35	2
NBS 120C	10	0.720	0.005	0.1	0.2	23	1
ASP 6 <sup>e</sup>	4	0.628	0.019	0.3	0.1	45	5
ASP 12 <sup>e</sup>	2	0.677	0.009	0.5	0.3	31	2

a

Number of samples measured.

b

Given in the absolute reference frame (ARF) of [Dennis et al. \(2011\)](#).

c

1 standard error.

d

Apparent clumped-isotope-based temperature calculated using Eq. [\(A1\)](#).

e

Produced larger quantities of CO<sub>2</sub> than other experiments and thus excluded from all discussion in case of contamination by exogenous carbonate phases not removed during acid washing.

$\Delta_{47}$  values are reported in the 'absolute' reference frame, or as it is sometimes referred to, the 'carbon dioxide equilibrium scale' of [Dennis et al. \(2011\)](#). This reference frame was generated by measuring gases isotopically equilibrated with water at 25 °C and gases heated in [quartz](#) glass tubes at 1000 °C. An acid digestion fractionation factor of 0.092‰ ([Henkes et al., 2013](#)) was used to convert measured  $\Delta_{47}$  values of CO<sub>2</sub> extracted from carbonate apatite at 90 °C to the 25 °C acid-digestion reference frame used for interlaboratory comparisons and clumped-isotope temperature calculations. The choice of the acid-digestion correction is discussed in Section A1. All phosphorite samples were run at least four times across at least three different analytical sessions, except for NBS 120C. NBS 120C samples were run in the same analytical session before our lab began regularly running 25 °C equilibrated gases in order to report samples in the absolute reference frame. We calculated the absolute reference frame values for measurements of this sample following the procedures for a 'secondary' absolute reference frame outlined in [Dennis et al. \(2011\)](#).

Phosphorite samples were screened for possible contamination that might result in isobaric interferences at mass 47 by measuring  $\Delta_{48}$  values, where  $\Delta_{48} = ({}^{48}\text{R}/{}^{48}\text{R}^* - 1) \times 1000$  as defined and described in [Huntington et al. \(2009\)](#). All  $\Delta_{48}$  values for data reported here are less than 0.6‰ ([Table 2](#)), which is below the commonly applied threshold value of ~1‰ for the rejection of analyses (e.g., [Henkes et al., 2013](#)). For comparison, the inorganic carbonate standards measured in this study have  $\Delta_{48}$  values that range from 0.4‰ to 0.6‰. These values are similar to the theoretical values expected for internal isotopic equilibrium for temperatures from 25 to 300 °C, which are 0.2–0.3‰ respectively ([Guo et al., 2009](#)).

Precision and accuracy for analyses of crystalline carbonate standards analyzed concurrently with phosphates were evaluated by running two standards, a Carrara marble in-house standard and [travertine](#) in-house standard (TV01), in every analytical session. Average  $\Delta_{47}$ ,  $\delta^{18}\text{O}$  and  $\delta^{13}\text{C}$  values and precisions for these standard are given

in [Tables A1](#) and [A2](#). Isotopic values for standards were found to be accurate: all averages are within 1 standard deviation of long term in-house values and, for Carrara Marble, values from other labs ([Dennis et al., 2011](#)).  $\Delta_{47}$  of standards are all within 1–2 standard errors of their accepted values ([Table A1](#)).  $\Delta_{47}$  standard deviations of carbonate standards in this study range from 0.013‰ to 0.017‰. These values are similar to, though slightly elevated over that expected from counting statistics ( $\sim 0.01\%$ ). Additionally, these standard deviations are similar to those published previously for carbonate standards measured at Caltech (0.013–0.03‰; [Dennis et al., 2011](#)) and elsewhere (0.01–0.038‰; [Dennis et al., 2011](#)). Standard deviations for  $\delta^{18}\text{O}$  were 0.07–0.10‰ and for  $\delta^{13}\text{C}$  were 0.02–0.05‰. These values are typical for measurements made at Caltech.

Phosphorite samples have similar, but slightly elevated (i.e., worse) experimental reproducibility as compared to the carbonate standards — apatites have  $\delta^{18}\text{O}$  standard deviations that are 0.14–0.17‰ higher than our carbonate standards and 0.004–0.008‰ higher for  $\Delta_{47}$  measurements ([Tables A1](#) and [A2](#)). This decrease in external precision could be due to, for example, heterogeneities in the samples or a result of a poorer performance of the acid digestion reaction for large phosphate samples. Regardless, the additional imprecision does not impact any of our interpretations. Two samples (ASP 6 and ASP 12) investigated gave high  $\text{CO}_2$  yields compared to other samples despite acid washing. Although there is nothing obviously exceptional with the isotopic data generated for these samples (they follow the same trends as other samples) they are not included in our discussion because it seems possible to us that they were contaminated by a carbonate-bearing phase other than apatite that was not removed with the acetic acid (e.g., dolomite).

All measured (including replicate)  $\delta^{13}\text{C}$ ,  $\delta^{18}\text{O}$ , and  $\Delta_{47}$  values for phosphorite samples and carbonate standards are given in [Supplementary Tables 1 and 2](#).

#### 2.4. Sample cleaning experiments

Cleaning experiments were performed to ensure calcite could be quantitatively removed without modifying a sample's  $\delta^{18}\text{OCO}_3$ ,  $\delta^{13}\text{CCO}_3$ , and  $\Delta_{47}$  values. A phosphorite sample from Florida, obtained from the Caltech mineralogical collection, was used for these experiments. This sample was reacted with either deionized water, buffered acetic acid (0.1 M, pH = 4.5), or triammonium [citrate](#) (0.5 M, pH = 0.5). Additionally, for some experiments, a spike of Carrara marble was added such that the spike was 5% by weight of the sample. These spiked samples were additionally reacted in either acetic

acid or triammonium citrate for 4 h, 24 h, or 48 h respectively. In no experiments were samples first pretreated with H<sub>2</sub>O<sub>2</sub>.

## 2.5. Conversion of $\Delta_{47}$ values to temperature

All  $\Delta_{47}$  values (in the absolute reference frame) were converted into ‘apparent equilibrium’ temperatures or ‘fictive’ temperatures ([Zhang, 1994](#)), which we term here  $\Delta_{47}$ -based temperatures or T $\Delta_{47}$ , using  $\Delta_{47}$  values. There currently exist multiple calibrations for conversion of  $\Delta_{47}$  values in the absolute reference frame into apparent equilibrium temperatures ([Dennis et al., 2011](#), [Eagle et al., 2013](#), [Henkes et al., 2013](#), [Zaarur et al., 2013](#), [Wacker et al., 2014](#), [Defliese et al., 2015](#), [Kluge et al., 2015](#)). Problematically, these calibrations differ in temperature sensitivity for  $\Delta_{47}$  measurements (‰/°C) by factors of up to 2. The cause of these differences is not known. It is not obviously related to sample preparation differences ([Wacker et al., 2014](#), [Defliese et al., 2015](#)). Furthermore, in the few cases where the same samples were measured in different labs, the  $\Delta_{47}$  values obtained were statistically indistinguishable ([Dennis et al., 2011](#)). Thus, the choice of which calibration to use is not straightforward.

We have chosen to use a slightly modified version (see Section A1 and Eq. [\(A1\)](#)) of the original temperature vs.  $\Delta_{47}$  calibration of [Ghosh et al. \(2006\)](#) translated into the absolute reference by [Dennis et al. \(2011\)](#) for the following two reasons: (i) this calibration was generated in the Caltech laboratory where all measurements reported here were made, though at 25 °C for acid digestions as opposed to 90 °C as they are currently done. And (ii) apatite samples from bioapatite fossil material ranging in known formation temperatures from 24 °C to 37 °C yield  $\Delta_{47}$ -based temperatures using a 90 °C acid digestion and the [Ghosh et al. \(2006\)](#) calibration that are within 1 standard error (s.e.) of the known formation temperatures in all cases ([Eagle et al., 2010](#)). We note that the use of the other calibrations does not change any first-order conclusions made here.

Additionally all reported clumped-isotope-based temperatures are within the range of temperatures used in the calibration of [Ghosh et al. \(2006\)](#), 1–50 °C, except for one sample which is within 1 s.e. of 50 °C ( $51 \pm 3$ , 1 s.e.). Thus, the possible inaccuracies associated with extrapolating the Ghosh et al. calibration to temperatures outside its range of calibration are not factors here.

Finally, implicit in using any of the clumped-isotope calibrations discussed above, which are all based on carbonate minerals (e.g., calcite, [aragonite](#), or dolomite), is that carbonate groups dissolved in apatites share an identical  $\Delta_{47}$ -vs. temperature relationship with the carbonate minerals used in the calibration. As discussed and demonstrated in [Eagle et al. \(2010\)](#) and [Stolper and Eiler \(2015\)](#), this appears, empirically, to be a robust assumption for samples with formation temperatures from ~25 to ~700 °C. This

assumption is further supported by theoretical calculations that indicate carbonate groups in apatite vs. in other carbonate groups share an indistinguishable  $\Delta_{47}$  vs. temperature relationship ([Eagle et al., 2010](#)).

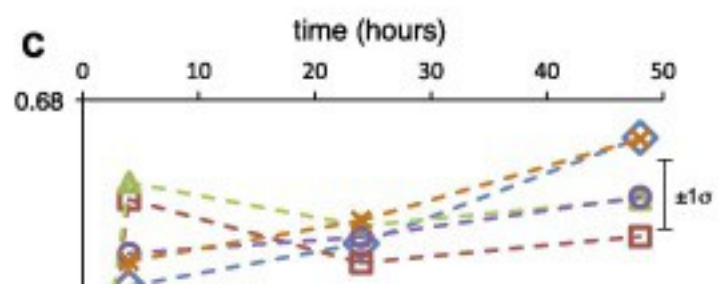
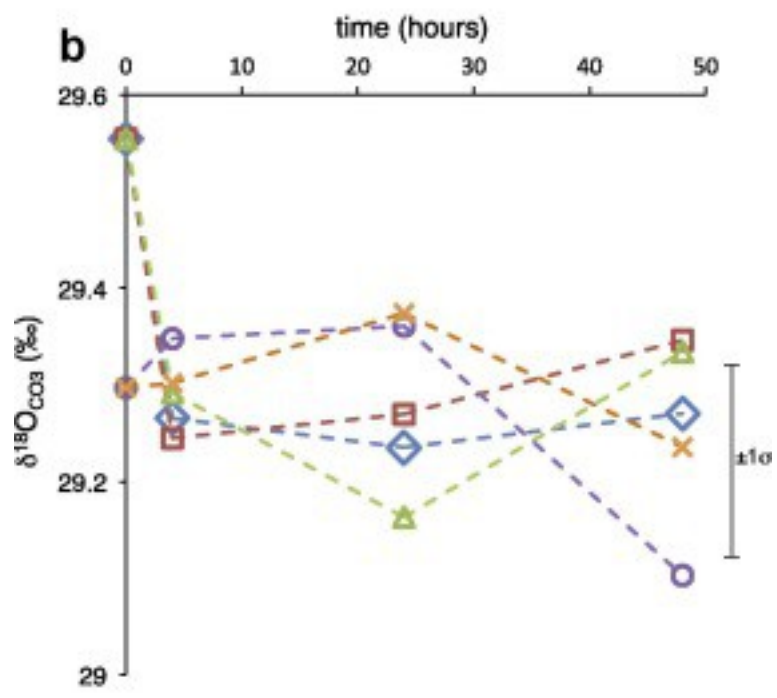
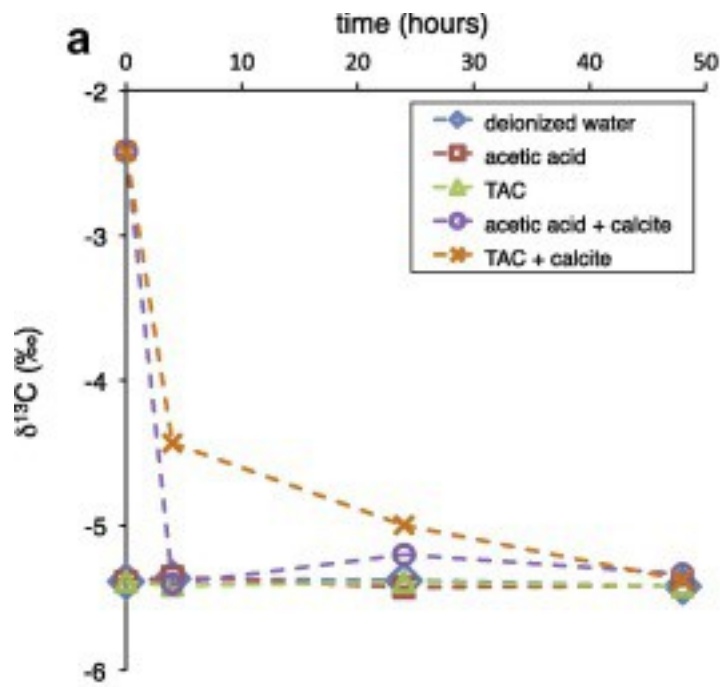
### 3. Results of acid washing experiments

A challenge with making clumped-isotope measurements on [carbonate groups](#) dissolved in [apatite](#) is that a large amount of sample is needed for each analysis: ~100 mg of apatite compared to 8 mg of [calcite](#). Thus, a critical concern for our analyses is the contamination of samples by small amounts (e.g., weight percent) of exogenous carbonate minerals. To deal with this, previous studies have used weak acids like [acetic acid](#) and triammonium [citrate](#) (TAC) to dissolve calcite and [aragonite](#), but leave apatite isotopically undisturbed ([Silverman et al., 1952](#), [Kolodny and Kaplan, 1970](#), [Shemesh et al., 1988](#), [Koch et al., 1997](#), [Eagle et al., 2010](#), [Stolper and Eiler, 2015](#)). Although these acids have been used to clean apatites for  $\delta^{18}\text{O}$  and  $\delta^{13}\text{C}$  measurements, their effects on  $\Delta_{47}$  values are not fully constrained — [Eagle et al. \(2010\)](#) and [Stolper and Eiler \(2015\)](#) showed that acetic acid does not appear to change  $\Delta_{47}$  values of carbonate groups in fossil material or igneous apatites. However, the samples used in the experiments of [Eagle et al. \(2010\)](#) and [Stolper and Eiler \(2015\)](#) were not known to contain contaminants. Consequently, how acid washes affect  $\Delta_{47}$  values when contaminants are present is not known. To address this, we measured the effects of acid washing on  $\Delta_{47}$  values using TAC, acetic acid, or deionized water on a [phosphorite](#) sample from the Caltech mineralogical collection with and without additions (i.e., spikes) of calcite (see Section [2.4](#) above).

#### 3.1. Washing without calcite spikes

We present the results of these acid-washing experiments in [Fig. 1](#) and [Table 3](#). First, we discuss the results in samples that were not spiked with calcite. Interestingly and unexpectedly, washing samples in deionized water has an effect on both the measured  $\delta^{18}\text{O}$  and  $\Delta_{47}$  values. Specifically, within the first 4 h of washing in deionized water, samples plateau to constant (within error)  $\delta^{18}\text{OCO}_3$ ,  $\delta^{13}\text{CCO}_3$ , and  $\Delta_{47}$  values ([Fig. 1](#)). We interpret this change then stabilization to indicate the dissolution and thus removal of a contaminant. We do not know what contaminant is being removed in the water, but we hypothesize it causes a mass-spectrometric interference at mass 46, raising the sample's  $\delta^{18}\text{OCO}_3$  value and thus lowering the  $\Delta_{47}$  value ([Fig. 1](#)). Water washing vs. acid washing in TAC or acetic acid appears to yield indistinguishable isotopic values (within analytical error) after 4 h of treatment. This suggests that once this contaminant is

dissolved, acid washing is no different from soaking samples in water. Additionally, this experiment shows the importance of rinsing all phosphorite (and perhaps other) samples before making isotopic measurements.



1. [Download high-res image \(262KB\)](#)
2. [Download full-size image](#)

Fig. 1. [Apatite](#) acid-cleaning experiments. TAC indicates triammonium [citrate](#). ‘+ calcite’ denotes addition of a Carrara marble spike to the experiment such that the spike was 5% by weight of the sample. (A) Effect of different acid washes on  $\delta^{13}\text{C}$  values of  $\text{CO}_3^{2-}$  groups liberated from a [phosphorite](#) standard. All samples converge to the same value, within error, by 48 h. Error bars of the measurement are smaller than the symbols. (B) Effect of different acid washes on  $\delta^{18}\text{O}$  values of  $\text{CO}_3^{2-}$  groups liberated from a phosphorite standard. All samples converge to the same value, within error, by 48 h. Given error bar is the typical  $\pm 1$  standard deviation of the measurement. See A for legend. (C) Effect of different acid washes on  $\Delta_{47}$  values of  $\text{CO}_3^{2-}$  groups liberated from a phosphorite standard. All samples converge to the same value, within error, by 48 h. Given error bar is the typical  $\pm 1$  standard deviation of the measurement. See A for legend.

Table 3. Acid washing experiments.

Sample	$\delta^{13}\text{C}$ (‰) <sup>a</sup>
<b>Unwashed apatite starting material</b>	−5.39
<b>4 h deionized (DI) water</b>	−5.37
<b>24 h DI water</b>	−5.38
<b>48 h DI water</b>	−5.42
<b>4 h acetic acid</b>	−5.36
<b>24 h acetic acid</b>	−5.43
<b>48 h acetic acid</b>	−5.42
<b>4 h triammonium citrate (TAC)</b>	−5.42
<b>24 h TAC</b>	−5.39
<b>48 h TAC</b>	−5.42
-----	
<b>+ calcite<sup>c</sup> with unwashed apatite starting material</b>	−2.42
<b>+ calcite 4 h acetic acid</b>	−5.40
<b>+ calcite 24 h acetic acid</b>	−5.20
<b>+ calcite 48 h acetic</b>	−5.33
<b>+ calcite 4 h TAC</b>	−4.43
<b>+ calcite 24 h TAC</b>	−5.00
<b>+ calcite 48 h TAC</b>	−5.38

<sup>a</sup> Referenced to the VPDB scale.

<sup>b</sup> Referenced to VSMOW.

<sup>c</sup> Given in the absolute reference frame (ARF) of [Dennis et al. \(2011\)](#).

<sup>d</sup> 1 standard error.



° Denotes addition of [calcite](#) material to the experiment.

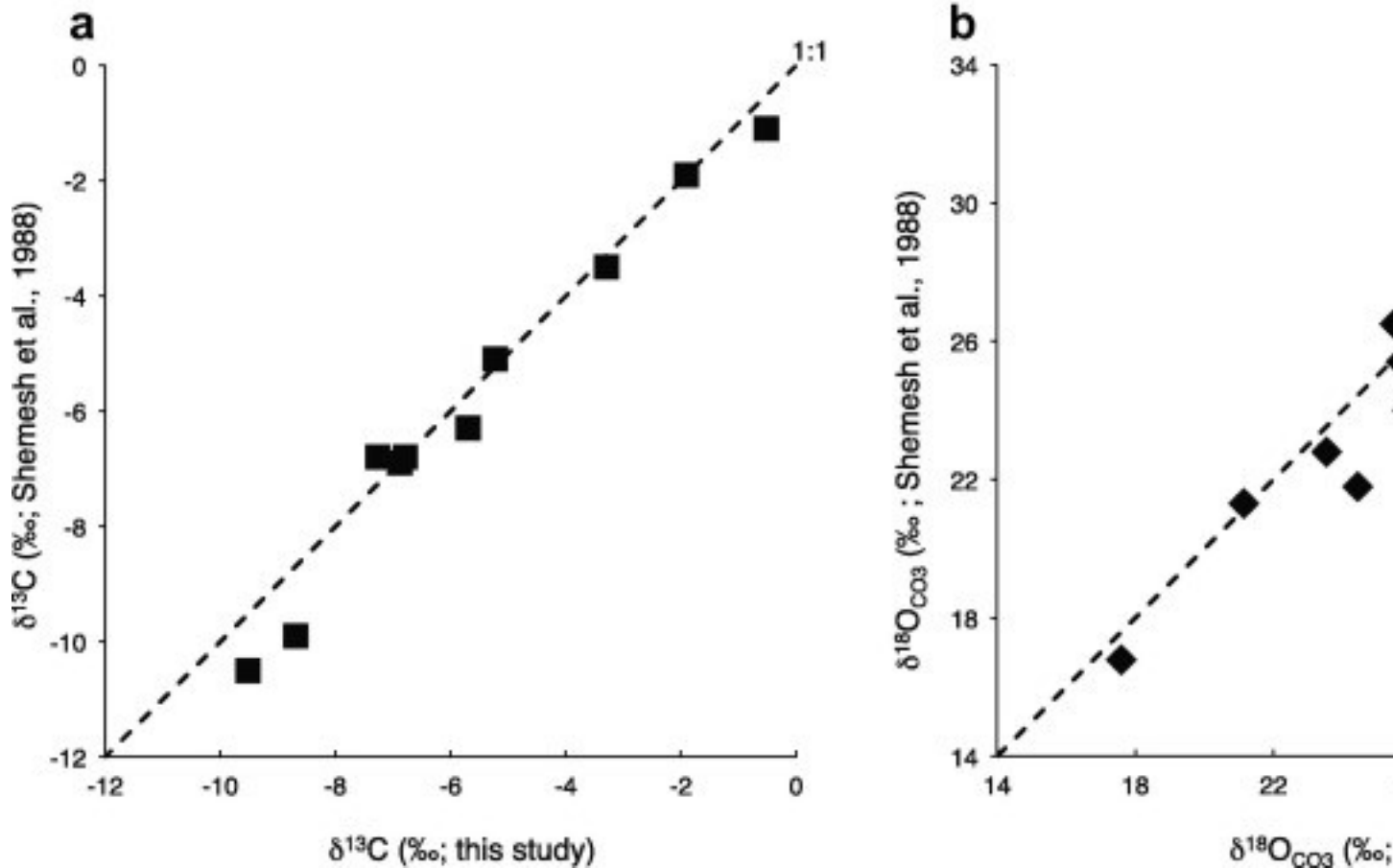
### 3.2. Washing with calcite spikes

The addition of aliquots of Carrara marble to the samples without subsequent acid washing causes a change in  $\delta^{13}\text{C}$  and  $\Delta_{47}$  values as would be expected. The  $\delta^{18}\text{O}$  value of the marble-spiked samples is the same as the unwashed, unspiked samples and thus is not useful for monitoring the removal of the carbonate spike. Regardless, the measurements of  $\delta^{13}\text{C}$  and  $\Delta_{47}$  demonstrate that acetic acid removes the calcite spike within 4 h, while TAC removes it within 48 h ([Fig. 1](#)). Based on these experiments, we chose to use a 48-h acetic-acid wash for all samples.

## 4. Phosphorite data

4.1. Comparison of measurements to those in [Shemesh et al. \(1988\)](#) and first-order observations based on the isotopic compositions

Data for all [phosphorite](#) samples are given in [Tables 1](#) and [2](#), including  $\Delta_{47}$ ,  $\delta^{13}\text{CCO}_3$ , and  $\delta^{18}\text{OCO}_3$  values measured in this study and  $\delta^{18}\text{OPO}_4$ ,  $\delta^{13}\text{CCO}_3$  and  $\delta^{18}\text{OCO}_3$  values previously measured in [Shemesh et al. \(1988\)](#). We first compared our measurements of  $\delta^{13}\text{CCO}_3$  and  $\delta^{18}\text{OCO}_3$  values to those given in [Shemesh et al. \(1988\)](#) in [Fig. 2](#). The comparison of measurements of both  $\delta^{13}\text{CCO}_3$  and  $\delta^{18}\text{OCO}_3$  from the two studies defines trends that are statistically indistinguishable from 1:1 lines passing through the origin of the respective plots: The best-fit linear regression slope and intercept for the  $\delta^{13}\text{CCO}_3$  comparison are  $1.05 \pm 0.06$  (1 standard deviation,  $\sigma$ ) and  $0.0 \pm 0.4$  ( $1\sigma$ ) respectively. For the  $\delta^{18}\text{OCO}_3$  comparison, the best-fit linear regression slope and intercept are  $0.94 \pm 0.08$  ( $1\sigma$ ) and  $0.8 \pm 2.0$  ( $1\sigma$ ). Consequently, we conclude that there are no systematic offsets between the measurements from the two labs. We note, though, that there is scatter beyond the stated error for each point around the 1:1 line for both measurements ([Fig. 2](#)). This scatter may be due to heterogeneities in the samples or perhaps due to different methodologies used — [Shemesh et al. \(1988\)](#) released  $\text{CO}_2$  from apatites using an [acid digestion](#) at 25 °C in McCrea-style reactors ([McCrea, 1950](#)) while we used a common acid bath held at 90 °C with continuous trapping of evolved  $\text{CO}_2$  at [liquid nitrogen](#) temperatures.



1. [Download high-res image \(172KB\)](#)
2. [Download full-size image](#)

Fig. 2. Comparison of bulk isotopic measurements of  $\text{CO}_3^{2-}$  groups in [phosphorites](#) from this study compared to those measured by [Shemesh et al. \(1988\)](#). Plotted lines are 1:1 lines that pass through the origin. (A) Comparison of  $\delta^{13}\text{C}_{\text{CO}_3}$  measurements. (B) Comparison of  $\delta^{18}\text{O}_{\text{CO}_3}$  measurements. Error bars are smaller than the symbols.

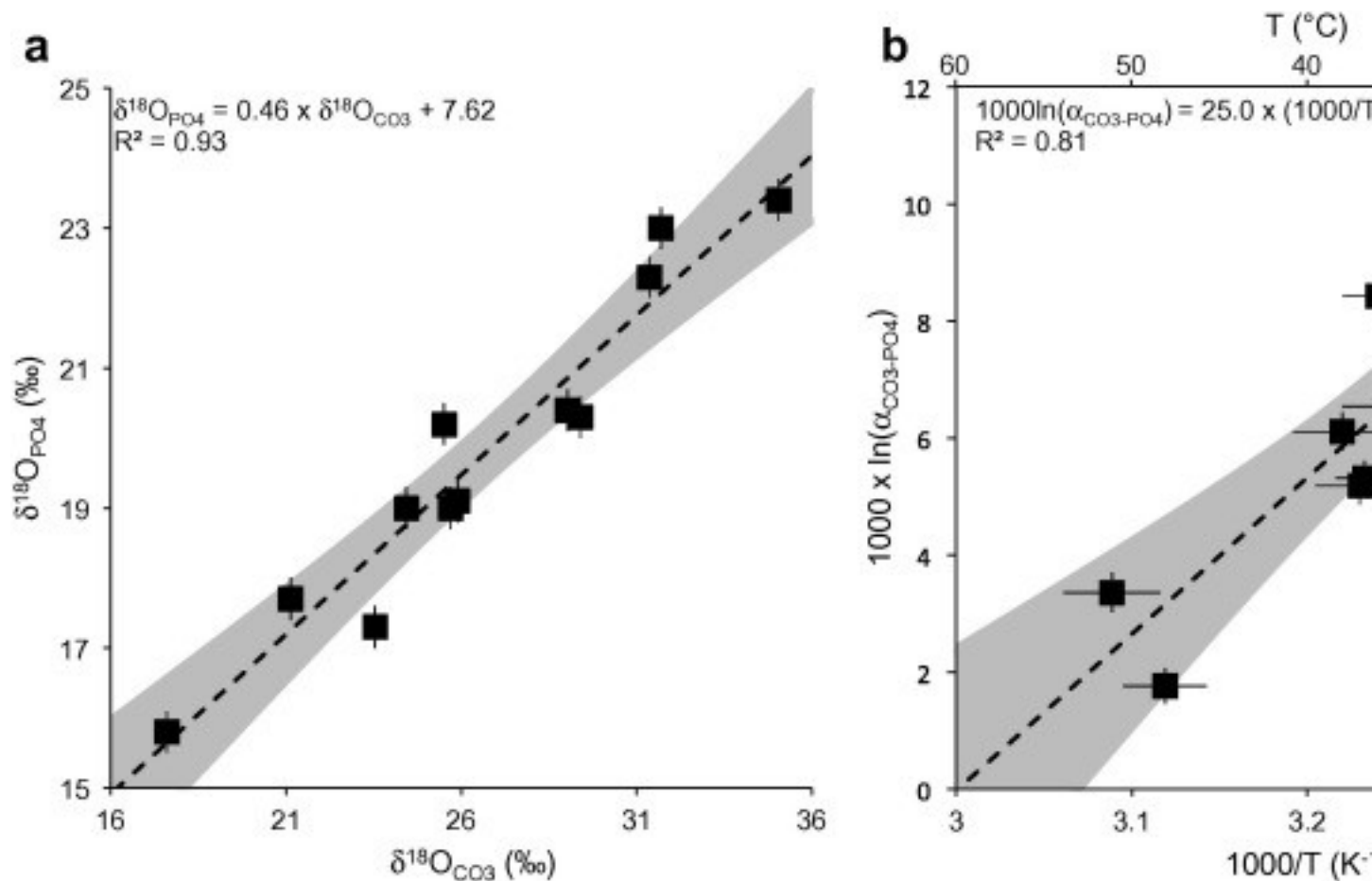
$\delta^{13}\text{C}$  values of [carbonate groups](#) in the measured apatites tend to be lower as compared to typical values for [Phanerozoic](#) marine carbonates ( $\delta^{13}\text{C} \approx 2 \pm 4\text{‰}$ ; [Lasaga, 1989](#)), ranging in value from  $-0.5\text{‰}$  to  $-9.5\text{‰}$ . These ranges are similar to those observed in apatite-bound carbonate groups in other phosphorites ([McArthur et al., 1980](#), [McArthur et al., 1986](#), [Birch et al., 1983](#), [Shemesh et al., 1983](#), [Shemesh et al., 1988](#), [Kastner et al., 1990](#), [Jarvis, 1992](#), [Sadaqah et al., 2007](#), [Baioumy et al., 2007](#)). Low  $\delta^{13}\text{C}$  values in phosphorites are often attributed to the incorporation of carbonate groups generated in sedimentary [pore waters](#) by the respiration of organic matter, which is typically lower in  $\delta^{13}\text{C}$  ( $\delta^{13}\text{C} \approx -25\text{‰}$ ) than marine carbonates (e.g., [McArthur et al., 1986](#)).

$\delta^{18}\text{O}_{\text{PO}_4}$  values of the sample suite (taken from [Shemesh et al., 1988](#)) range from  $15.8\text{‰}$  to  $23.4\text{‰}$ . For comparison, in modern (i.e.,  $\sim <100,000$  year old) phosphorites,

$\delta^{18}\text{OPO}_4$  values range from 21.7‰ to 24.8‰ ([Shemesh et al., 1983](#), [Shemesh et al., 1988](#)). The  $\delta^{18}\text{OCO}_3$  values we measured for these samples range from 17.6‰ to 35‰ while modern phosphorites tend to range from 30.5‰ to 33.6‰ ([Kolodny and Kaplan, 1970](#), [Shemesh et al., 1983](#), [Shemesh et al., 1988](#)). Thus, many of the samples exhibit [oxygen isotope](#) values outside of the range observed in recent phosphorites, with most samples lower in both  $\delta^{18}\text{OPO}_4$  and  $\delta^{18}\text{OCO}_3$  than generally encountered today or the recent past.

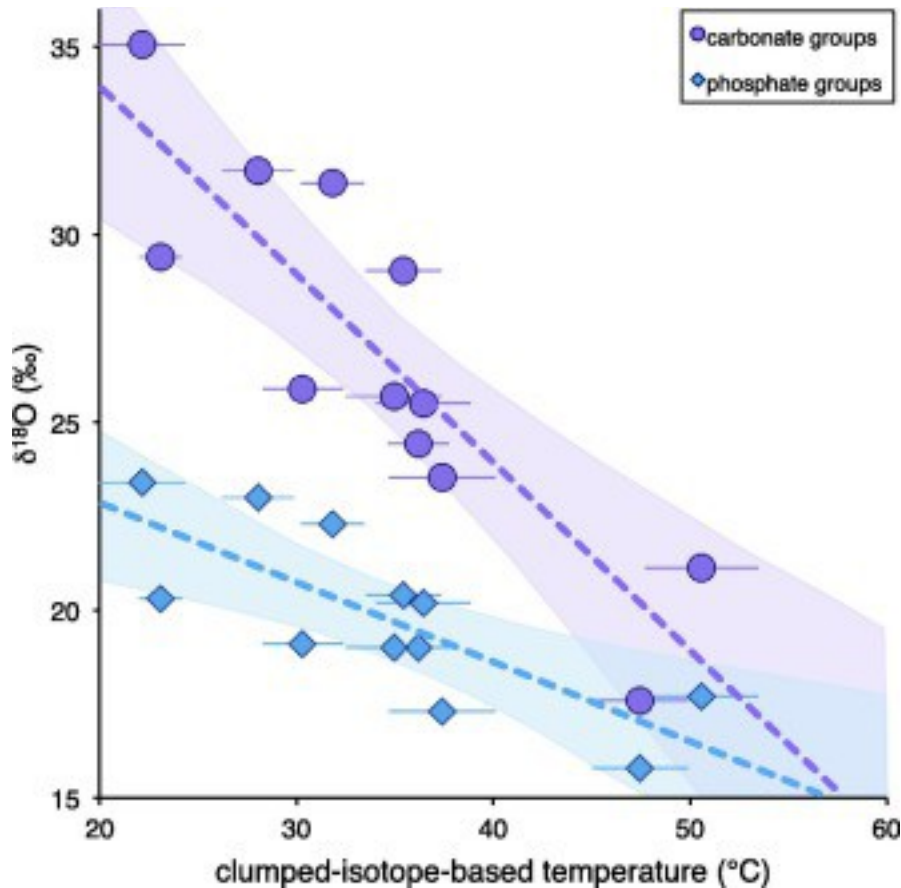
$\Delta_{47}$  values in the absolute reference frame range from 0.613‰ to 0.724‰. These correspond to  $\Delta_{47}$ -based temperatures of 22–51 °C — i.e., from plausible [earth-surface](#) temperatures to temperatures that presumably reflect either: (i) kinetic [isotope effects](#) during precipitation (e.g., [Ghosh et al., 2006](#), [Affek et al., 2008](#), [Daëron et al., 2011](#), [Saenger et al., 2012](#)); (ii) mixing between carbonate groups formed in or brought to isotopic equilibrium (and thus at homogenous phase equilibrium) but incorporated into the [apatite](#) over a range of temperatures during different diagenetic events; or (iii) intra-mineral, closed-system isotope-exchange reactions ([Ghosh et al., 2006](#), [Dennis and Schrag, 2010](#), [Passey and Henkes, 2012](#), [Henkes et al., 2014](#), [Stolper and Eiler, 2015](#)). We evaluate these possibilities in the next section (Section [4.2](#)).

Two correlations are present in the data: First,  $\delta^{18}\text{OCO}_3$  and  $\delta^{18}\text{OPO}_4$  values are linearly correlated with each other, with the best-fit line having a slope of  $0.46 \pm 0.05$  ( $1\sigma$ ) ([Fig. 3a](#)). This is similar to, but just statistically distinct at the  $2\sigma$  level, from the previously observed slope of 0.57 ([Shemesh et al., 1988](#)). This difference is possibly related to the additional samples examined by [Shemesh et al. \(1988\)](#) that were not measured here, including various [Cenozoic](#) samples with elevated ( $>23\%$ )  $\delta^{18}\text{OPO}_4$  values. Second,  $1000 \times \ln(\alpha_{\text{CO}_3\text{-PO}_4})$  values are linearly correlated with the measured clumped-isotope temperatures, expressed as  $1000/T$ , where  $T$  is temperature in Kelvin ([Fig. 3b](#);  $\alpha_{a-b} = [1000 + \delta_A]/[1000 + \delta_B]$ ), with a slope of  $25.0 \pm 6.1$  ( $1\sigma$ ) and intercept of  $-74.2 \pm 25.1$  ( $1\sigma$ ). These correlations can be seen alternatively by plotting  $\Delta_{47}$  vs.  $\delta^{18}\text{OCO}_3$  and  $\delta^{18}\text{OPO}_4$  ([Fig. 4](#)). As expected, linear correlations exist in these composition spaces as well.



1. [Download high-res image \(211KB\)](#)
2. [Download full-size image](#)

Fig. 3. (A) Relationship between  $\delta^{18}\text{O}_{\text{PO}_4}$  values given in [Shemesh et al. \(1988\)](#) vs.  $\delta^{18}\text{O}_{\text{CO}_3}$  values measured in this study. B) Relationship between  $1000 \times \ln(\alpha_{\text{CO}_3\text{-PO}_4})$  vs.  $1000/T$  where T, in Kelvin, is the derived clumped-isotope-based temperature.  $\alpha_{\text{CO}_3\text{-PO}_4}$  values are calculated as  $(1000 + \delta^{18}\text{O}_{\text{CO}_3}) / (1000 + \delta^{18}\text{O}_{\text{PO}_4})$ . Error bars of data are  $\pm 1$  standard error. Gray area outlines the 95% confidence interval of the linear, least-squares regression given by the dotted black lines.



1. [Download high-res image \(148KB\)](#)
2. [Download full-size image](#)

Fig. 4. Comparison of  $\delta^{18}\text{O}_{\text{CO}_3}$  vs. the clumped-isotope ( $\Delta_{47}$ -based) temperature and of  $\delta^{18}\text{O}_{\text{PO}_4}$  vs. the clumped-isotope-based temperature. Both show linear correlations. Best fit lines are given as dotted lines with 95% confidence intervals as the shaded regions. We note that this is simply a different way of looking at the data presented in [Fig. 3](#).

#### 4.2. Evaluation of intramineral thermodynamic equilibrium

##### 4.2.1. Can $\Delta_{47}$ -based temperatures record mineral formation temperatures?

A key question is how to interpret the  $\Delta_{47}$ -based temperatures of the samples. For example, are the measured temperatures mineral formation/recrystallization temperatures? This would require the carbonate groups to have been in homogenous [phase equilibrium](#) during mineral formation/recrystallization. This assumption was taken by [Bradbury et al. \(2015\)](#): They observed  $\Delta_{47}$ -based temperatures of 61 °C in two samples and 66 °C in another sample ( $\pm 5$  °C 1 s.e. for all three) in apatites from phosphorites in the Monterey Formation. These temperatures are clearly too high to be the actual phosphorite formation temperatures. Consequently, [Bradbury et al. \(2015\)](#) interpreted the clumped-isotope temperatures as the temperatures at which

the apatites recrystallized (or were otherwise diagenetically modified). This interpretation requires that any resetting of clumped-isotope temperatures via [diagenesis](#) occurred at a single temperature in a process that allowed all carbonate groups in the phosphorite to obtain a new internal isotopic equilibrium.

Thus, a critical question is whether phosphorite  $\Delta_{47}$ -based temperatures, before potential post-depositional modification, record mineral formation temperatures. Or, alternatively, are the  $\Delta_{47}$  values controlled by kinetic isotope effects? If so, the measured temperatures would be unrelated (or related through processes other than the equilibrium relationship) to environmental formation temperatures. This is important to evaluate because formation in isotopic equilibrium would allow phosphorites to be used for [paleotemperature](#) reconstructions of formational and perhaps diagenetic environments. Evaluation of this requires samples with independently constrained formation temperatures. Problematically, independent constraints on mineral formation temperatures do not exist for the majority of samples given their geologically ancient age (multiple millions of years).

ASP 22, the likely youngest sample examined (1–5 million years old; [Table 1](#)), may provide some useful constraints. This sample, from off the coast of Namibia, is identified in [Shemesh \(1990\)](#) as a glauconized pelletal phosphorite. These glauconized pelletal phosphorites are hypothesized to have formed in evaporitic onshore [estuary](#) environments ([Bremner and Rogers, 1990](#)). Although the temperatures in these ancient estuaries are not known, modern [sea-surface temperatures](#) in the area are  $\sim 18^\circ\text{C}$  ([Gammelsrød et al., 1998](#)). This temperature is within  $2\sigma$  of the measured  $\Delta_{47}$ -based temperature of ASP-22,  $22^\circ\text{C}$  ( $\pm 2$ , 1 s.e.) and thus could represent plausible mineral formation temperatures. Based on this result, we suggest and proceed with the assumption that  $\Delta_{47}$ -based temperatures of unmodified phosphorites can reflect mineral formation temperatures and thus that there is no obvious presence of kinetic isotope effects affecting clumped-isotope compositions during mineral formation. However, this remains a hypothesis and future work should test this interpretation by examining modern phosphorite deposits with well-constrained formation temperatures.

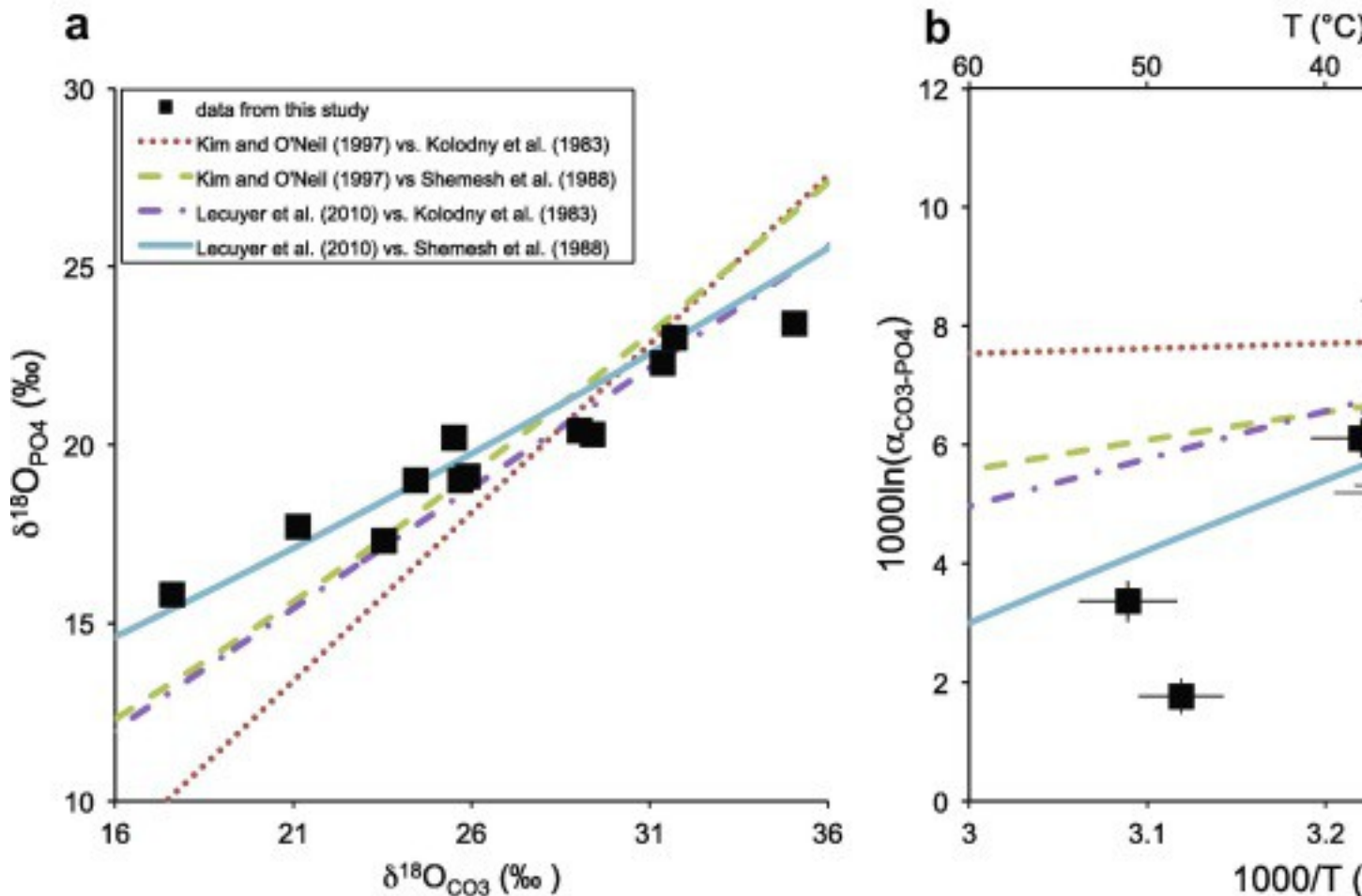
4.2.2. Do the  $\delta^{18}\text{OPO}_4$  and  $\delta^{18}\text{OCO}_3$  values and clumped-isotope temperatures reflect the formation/recrystallization temperatures of the phosphorites?

Next, we examined whether the trends in [Fig. 3](#) are consistent with formation of apatites in oxygen-isotope equilibrium between  $\text{PO}_4^{3-}$  and  $\text{CO}_3^{2-}$  groups and internal isotopic equilibrium between carbonate groups for clumped isotopologues. This was done using experimentally derived oxygen-isotope [fractionation](#) factors (the  $\alpha$  above) between carbonate and water and between phosphate and water. Multiple phosphate-water

fractionation factors exist and need to be considered ([Kolodny et al., 1983](#), [Karhu and Epstein, 1986](#), [Shemesh et al., 1988](#), [Lécuyer et al., 1996](#), [Lécuyer et al., 2013](#), [Pucéat et al., 2010](#)). As all but one of the samples measured here was made on BiPO<sub>4</sub> ([Kolodny et al., 1983](#)), we only considered calibrations generated using the BiPO<sub>4</sub> method. After examining the relevant calibrations, we chose two equilibrium phosphate-water oxygen-isotope fractionation calibrations for this test: the low temperature calibration (<25 °C) of [Kolodny et al. \(1983\)](#) and the high temperature (<510 °C) calibration of [Shemesh et al. \(1988\)](#). We did not include the calibration of [Longinelli and Nuti \(1973\)](#) as it is identical within error to that of [Kolodny et al. \(1983\)](#). Additionally, we did not include the calibration of [Karhu and Epstein \(1986\)](#) because the high-temperature datum from this study is included in the [Shemesh et al. \(1988\)](#) calibration. We note that some caution should be taken when using the [Shemesh et al. \(1988\)](#) calibration for two reasons: First, one of the high-temperature (>350 °C) data points was taken from [Karhu and Epstein \(1986\)](#) and this sample has an estimated (350 °C) as opposed to known formation temperature. Second, the other high-temperature (510 °C) data point used to calibrate the phosphate-water oxygen-isotope fractionation factor vs. temperature from the [Shemesh et al. \(1988\)](#) study implies the presence of a so-called 'crossover' in the calibration ([Stern et al., 1968](#)). Specifically, all low-temperature (e.g., from the surface of the earth) phosphates formed in isotopic equilibrium have δ<sup>18</sup>O values that are greater than the δ<sup>18</sup>O values of the fluid from which they precipitated. However, the highest temperature (510 °C), experimentally derived apatite has a δ<sup>18</sup>O value that is lower than a fluid would have if it were isotopically equilibrated with the mineral. The presence of this crossover makes use of a linear 1/T<sup>2</sup> form for the [temperature dependence](#) of the fractionation factor, which is the form used in the [Shemesh et al. \(1988\)](#) calibration, potentially incorrect. This is because the trend may not be linear between the high temperature and low temperature points used for the calibration ([Stern et al., 1968](#)). Regardless, we considered this calibration as it is found in the literature and includes calibration points at elevated (>25 °C) temperatures.

We compared these phosphate-water calibrations to two separate carbonate-water fractionation factors for four total comparisons. The first carbonate-water calibration used is the [Kim and O'Neil \(1997\)](#) calibration for [calcite](#). Although carbonate groups in apatite are distinct from those in calcite, calcite-based fractionation factors have been used in the past to interpret the meaning of carbonate [oxygen isotopes](#) in phosphates (e.g., [Shemesh et al., 1983](#), [Shemesh et al., 1988](#), [McArthur and Herczeg, 1990](#)). The second calibration is from [Lécuyer et al. \(2010\)](#) and is for carbonate groups substituted into [hydroxyapatite](#) in equilibrium with water.

We compared our results to the four different lines that can be produced from the calibrations described above in Fig. 5. In Fig. 5a, for the calculated relationships between  $\delta^{18}\text{O}_{\text{PO}_4}$  and  $\delta^{18}\text{O}_{\text{CO}_3}$  in apatite, we assumed mineral formation in waters with a  $\delta^{18}\text{O} = 0\text{‰}$ , which is the approximate average value of modern seawater. Using the estimated average isotopic composition of the ocean without continental ice sheets ( $-1.2\text{‰}$ ; Miller et al., 1987) does not change any conclusions. The isotopic composition of the water controls the vertical position of the lines in Fig. 5a. For example, changing the  $\delta^{18}\text{O}$  of the water in equilibrium with the minerals moves the position of the lines along a 1:1 line. Importantly, the  $\delta^{18}\text{O}$  of water has no effect on the slopes of the lines. In Fig. 5b,  $1000 \times \ln(\alpha_{\text{CO}_3\text{-PO}_4})$  vs.  $1000/T$  for the models is compared to the measured  $\Delta_{47}$ -based temperatures. Unlike in Fig. 5a, this space (Fig. 5b) is independent of the chosen isotopic composition of the water.



1. [Download high-res image \(292KB\)](#)
2. [Download full-size image](#)

Fig. 5. (a) Comparison of various theoretical lines for equilibrium between oxygen isotopes of  $\text{PO}_4^{3-}$  and  $\text{CO}_3^{2-}$  vs. the measured data. For the theoretical calculations,



samples are assumed to have equilibrated with waters with a  $\delta^{18}\text{O}$  value equal to 0‰: see text for details. (b) Comparison of theoretical lines for  $1000 \times \ln(\alpha_{\text{CO}_3\text{-PO}_4})$  vs.  $1000/T$  where T, in Kelvin, is the derived clumped-isotope temperature vs. the measured values.  $\alpha_{\text{CO}_3\text{-PO}_4}$  values are calculated as  $(1000 + \delta^{18}\text{OCO}_3)/(1000 + \delta^{18}\text{OPO}_4)$ . Theoretical lines for carbonate-water [fractionation](#) factors for  $\delta^{18}\text{OCO}_3$  values are given in [Kim and O’Neil \(1997\)](#) and [Lécuyer et al. \(2010\)](#). Theoretical lines for  $\text{PO}_4$ -water fractionation factors for  $\delta^{18}\text{OPO}_4$  values are given in [Kolodny et al. \(1983\)](#) and [Shemesh et al. \(1988\)](#). Error bars of data are  $\pm 1$  standard error.

In [Fig. 5a](#), the two lines defined by the combination of the [Kim and O’Neil \(1997\)](#) carbonate calibration with the phosphate calibrations of [Kolodny et al. \(1983\)](#) and the line defined by the combination of [Lécuyer et al. \(2010\)](#) with [Shemesh et al. \(1988\)](#) produce slopes that are steeper than the slope defined by the data trend. This was also observed by [Shemesh et al. \(1988\)](#) when attempting a similar exercise. If any of these lines are the correct combination of fractionation factors, it would suggest that, although some of the points may lie on or near lines that define isotopic equilibrium, many are significantly offset. Such offsets would indicate the presence of [disequilibrium](#) processes that have disturbed some samples away from oxygen-isotope equilibrium between the phosphate and carbonate groups. This was the conclusion of [Shemesh et al. \(1988\)](#).

Interestingly, the line in [Fig. 5a](#), which is based on combination of the [Lécuyer et al. \(2010\)](#) and [Shemesh et al. \(1988\)](#) calibrations, has a slope that is generally consistent with the trend of the data. Closer inspection, however, demonstrates that this line’s goodness of fit is fortuitous. Specifically, as discussed above, one sample examined here, ASP 22, has a well-constrained formational and burial history. This sample was dredged from the sea-floor (and thus experienced limited burial diagenesis) in waters with a temperature of  $\sim 12^\circ\text{C}$  ([Shemesh et al., 1983](#)) and likely formed at higher temperatures (see discussion in section [4.2.1](#)). However, the calculated temperature based on the  $\delta^{18}\text{OPO}_4$  and  $\delta^{18}\text{OCO}_3$  values and the [Lécuyer et al. \(2010\)](#) vs. [Shemesh et al. \(1988\)](#) fractionation factors is  $-8^\circ\text{C} \pm 3 (1\sigma)$ . This temperature is  $2\sigma$  below the modern freezing point of seawater,  $-2^\circ\text{C}$ , and significantly below the current [environmental temperatures](#). This demonstrates that despite the visual goodness of fit of the [Lécuyer et al. \(2010\)](#) vs. [Shemesh et al. \(1988\)](#) line in [Fig. 5a](#), the temperatures derived using this line do not yield a reasonable mineral formation temperature for the sample with the best constrained formation and diagenetic history. Based on this, we suggest, as concluded previously by [Shemesh et al. \(1988\)](#), that the  $\delta^{18}\text{O}$  values from the full suite of data examined are not consistent with the carbonate

and [phosphate groups](#) preserving mutual oxygen-isotope equilibrium at formation in the whole sample set for any of the examined  $\delta^{18}\text{O}$  vs. temperature calibrations for carbonate and phosphate groups. This does not indicate that all samples are isotopically modified, just that there are many samples that are isotopically disturbed away from  $\delta^{18}\text{O}$  equilibrium. This inference is further supported by comparison of the measured  $\Delta_{47}$ -based temperatures vs.  $1000 \times \ln(\alpha_{\text{CO}_3\text{-PO}_4})$  trend observed in [Fig. 3b](#) to the trends predicted by these calibrations ([Fig. 5b](#)). This comparison demonstrates that the measured  $\Delta_{47}$ -based temperatures are, in many cases, not the temperatures that would have been predicted based on the bulk oxygen isotopic compositions ( $\delta^{18}\text{OCO}_3$  and  $\delta^{18}\text{OPO}_4$ ) of the apatites and the various published calibrations. This is a particularly informative comparison because the positions of the lines in [Fig. 5b](#), unlike in [5a](#), are independent of the composition of the water in which the apatite formed. Thus, the lack of agreement between the  $\Delta_{47}$ -based temperatures and the predicted temperatures from the difference in  $\delta^{18}\text{O}$  between the carbonate and phosphate groups provides supporting and independent evidence that many apatites contain phosphate and carbonate groups that are out of mutual isotopic equilibrium.

As discussed above, the apparent mismatch between the observed  $\delta^{18}\text{OCO}_3$  and  $\delta^{18}\text{OPO}_4$  values vs. those expected for isotopic equilibrium was suggested by [Shemesh et al. \(1988\)](#) to be the result of diagenesis. Specifically, [Shemesh et al. \(1988\)](#) hypothesized that during burial, both the carbonate groups and phosphate groups partially exchanged oxygen with sedimentary fluids at either elevated temperatures or in waters with lower  $\delta^{18}\text{O}$  values. Additionally, they attributed the general shallowness of the slope for the data trend observed in [Figs. 3a](#) and [5a](#) compared to that expected for mutual isotopic equilibrium between phosphate and carbonate groups to be the result of different rates of oxygen-isotope exchange between water and phosphate groups vs. water and carbonate groups. Specifically, they suggested that the carbonate groups exchanged [oxygen atoms](#) more quickly with water than the phosphate groups did.

The clumped-isotope data support this diagenetic model because the temperatures measured correlate with the  $\delta^{18}\text{O}$  values of both the  $\text{CO}_3$  and  $\text{PO}_4$  groups ([Fig. 4](#)). Specifically, the higher clumped-isotope temperatures correspond to lower  $\delta^{18}\text{O}$  values for both the phosphate and carbonate groups. This correlation, as well as that between  $\delta^{18}\text{OPO}_4$  and  $\delta^{18}\text{OCO}_3$  ([Figs. 3a](#) and [5a](#)) suggests the presence of a process capable of lowering the  $\delta^{18}\text{O}$  values of both the carbonate and phosphate groups in concert while at the same time raising the measured  $\Delta_{47}$ -based temperatures. Such correlations can be explained through increasing degrees of diagenesis in a water-buffered system at

elevated temperatures. This would cause the measured clumped-isotope temperatures to increase while, at the same time, the  $\delta^{18}\text{O}$  values to decrease either due to the smaller difference in  $\delta^{18}\text{O}$  at isotopic equilibrium between water and carbonate and [phosphate minerals](#) at elevated temperatures ([Urey, 1947](#), [McCrea, 1950](#), [Epstein et al., 1953](#), [O'Neil et al., 1969](#), [Longinelli and Nuti, 1973](#), [Kolodny et al., 1983](#), [Kim and O'Neil, 1997](#), [Lécuyer et al., 2010](#)) or due to lower  $\delta^{18}\text{O}$  values of diagenetic fluids compared to the fluids present during mineral precipitation. In the next section, we take this hypothesis and develop a quantitative model to explicitly test its plausibility. Before exploring this model, we note that there is an alternative explanation for the presence of elevated  $\Delta_{47}$ -based temperatures ( $>\approx 30$  °C) relative to what would be expected for Earth-surface conditions in many of the samples: the  $\Delta_{47}$ -based temperatures could have been partially reset through closed-system isotope-exchange reactions mediated by solid-state short-range diffusion within the mineral lattice ([Ghosh et al., 2006](#), [Dennis and Schrag, 2010](#), [Passey and Henkes, 2012](#), [Henkes et al., 2014](#), [Stolper and Eiler, 2015](#)). This is plausible as, at least in the few high-temperature apatites measured from (igneous) carbonatites, the blocking temperature for the  $\Delta_{47}$ -based thermometer (i.e., the approximate temperature above which solid-state atomic mobility can reset the apparent temperature) may be as low as  $\sim 70$  to  $80$  °C in carbonate groups in apatite ([Stolper and Eiler, 2015](#)). However, this explanation does not provide an obvious mechanism for the co-variation between the measured clumped-isotope temperatures and the  $\delta^{18}\text{OCO}_3$  and  $\delta^{18}\text{OPO}_4$  values ([Fig. 3](#), [Fig. 4](#), and [5](#)) — closed-system isotope exchange will not cause the  $\delta^{18}\text{O}$  values of the phosphate groups (which buffer the isotopic composition of the apatite) to change. Consequently, as diagenesis can explain the co-variation between  $\delta^{18}\text{O}$  values of phosphate and the  $\Delta_{47}$ -based temperatures while closed-system isotope-exchange reactions cannot, we do not consider closed-system isotope-exchange processes further.

## 5. A diagenetic model for the isotopic composition of phosphorite apatite

### 5.1. The model

The divergence between the observed  $\delta^{18}\text{OCO}_3$  and  $\delta^{18}\text{OPO}_4$  values and  $\Delta_{47}$ -based temperatures from the relationships expected for mineral formation in isotopic equilibrium with water ([Fig. 5](#)) as well as their correlations with each other ([Figs. 3](#) and [4](#)) suggest that a non-equilibrium process is modifying both the bulk and clumped-isotopic compositions of some samples away from isotopic equilibrium. Furthermore, the correlations between  $\delta^{18}\text{OCO}_3$  and  $\delta^{18}\text{OPO}_4$  values ([Fig. 3a](#)) and the  $\Delta_{47}$ -based temperatures with both  $\delta^{18}\text{OCO}_3$  and  $\delta^{18}\text{OPO}_4$  ([Fig. 4](#)) requires that whatever

non-equilibrium processes is at work, it acts on both the [carbonate and phosphate groups](#) (and is generally regular in its behavior, despite our having examined samples from many different [geological times](#) and locations). A process that can accomplish this is the partial dissolution and reprecipitation of a sample over a range of temperatures and/or fluid [isotopic compositions](#) during burial in sediments. In such a case, a sample would consist of a mixture of diagenetic and original components. Although all mineral components, both diagenetic and original, may have formed in isotopic equilibrium with sedimentary [pore waters](#), the calculated temperature based on the difference in  $\delta^{18}\text{OPO}_4$  and  $\delta^{18}\text{OCO}_3$  as well as the  $\Delta_{47}$ -based temperature as measured on that mixture would not be interpretable as a physically meaningful formation/re-equilibration temperature. Instead this temperature would represent a mixture of signals originating from the original precipitation event and later [diagenesis](#). Although such measurements could lead to an interpretable signal, the process altering the original isotopic composition must be recognized and understood first. In this section we examine the consequences of such diagenetic reactions on the measured isotopic parameters. A key aspect of the diagenesis of apatites to consider is that during dissolution and reprecipitation reactions,  $\text{CO}_3^{2-}$  and  $\text{PO}_4^{3-}$  groups may exchange oxygen with waters at different rates. As discussed above, such a difference was originally suggested by [Shemesh et al. \(1988\)](#) as a key control on the correlation between  $\delta^{18}\text{OCO}_3$  and  $\delta^{18}\text{OPO}_4$  seen in [Fig. 3a](#). Furthermore, such differential reaction rates have been shown experimentally: In the absence of organisms, [phosphate groups](#) exchange [oxygen isotopes](#) with water more slowly than carbonate groups do. In contrast, in experiments that include organisms, phosphate groups in [apatite](#) exchange oxygen isotopes more rapidly with water than carbonate groups do ([Zazzo et al., 2004](#); see below). We explored the consequences of diagenetic reactions that promote exchange of oxygen-isotopes between phosphate and carbonate groups with water quantitatively using a model based on the kinetic framework described in [Criss et al. \(1987\)](#) and [Gregory et al. \(1989\)](#). This framework is designed to describe the kinetics of isotope-exchange reactions between multiple phases/species with water (or any other phase) and allows different phases to react at different rates. Note, however, that the model assumes reacting species follow equilibrium [fractionations](#); i.e., it is a kinetic model but does not involve kinetic [isotope effects](#). We used this framework to explore the trajectories that diagenesis creates during alteration of  $\delta^{18}\text{OCO}_3$ ,  $\delta^{18}\text{OPO}_4$  and  $\Delta_{47}$  values when carbonate and phosphate groups react at different rates in the composition spaces outlined in [Figs. 3 and 5](#).

Using the kinetic rate laws derived in [Criss et al. \(1987\)](#) and [Gregory et al. \(1989\)](#) for bulk [oxygen-isotope](#) exchange reactions in a water buffered system, it can be shown that:

$$(1) F_{PO4} = (F_{CO3}) k_{PO4} / k_{CO3}$$

In Eq. (1),  $F = ({}^{18}R_{\text{measured}} - {}^{18}R_{\text{equilibrium}}) / ({}^{18}R_{\text{initial}} - {}^{18}R_{\text{equilibrium}})$ , where the equilibrium value represents the final value after a sample has fully recrystallized and is in isotopic equilibrium with the fluid. 'k' is the rate constant for oxygen-isotope exchange between carbonate ( $k_{CO3}$ ) or phosphate ( $k_{PO4}$ ) with water. F can take on values from 1 to 0 where 1 indicates no reaction has taken place while 0 is complete reaction. This model was previously used by [Zazzo et al. \(2004\)](#) to quantify different isotope-exchange rates between carbonate and phosphate groups in apatite with water on ground-up (100–700 micron) fossil teeth and bone bioapatite (hydroxyapatite) with and without microorganisms. They found  $k_{PO4}/k_{CO3}$  ratios of 0.1 for abiotic experiments and 2–15 for biotic reactions.

In order to extend this model to clumped-isotope exchange reactions in carbonates (which to our knowledge has not been done) we made the following additional assumptions:

(i) We assumed that the kinetics of the changes in the clumped-isotope composition of the apatites can be described and modeled using  $\Delta_{47}$  values. This assumption holds if there is a constant offset between the carbonate's clumped isotopologue composition (dominated [97%] by the abundance of the mass 63 isotopologue,  ${}^{13}\text{C}^{16}\text{O}_2^{18}\text{O}$ ) and its  $\Delta_{47}$  value — this has been observed to be the case experimentally ([Ghosh et al., 2006](#), [Guo et al., 2009](#)). We note, though, that theoretical calculations indicate that  $\Delta_{47}$  values could be non-linear functions of a sample's carbonate clumped-isotope composition ([Guo et al., 2009](#)), but, as of yet, this has not been observed empirically.

(ii) We assumed that changes in abundances of mass 47 isotopologues ( ${}^{13}\text{C}^{16}\text{O}^{18}\text{O}$ ,  ${}^{12}\text{C}^{17}\text{O}^{18}\text{O}$ ,  ${}^{13}\text{C}^{17}\text{O}_2$ ) vs. mass 44 isotopologue ( ${}^{12}\text{C}^{16}\text{O}_2$ ) of the  $\text{CO}_2$  derived from the carbonate groups obey the following kinetic form, which is also based on the kinetic derivations described in [Criss et al. \(1987\)](#) and [Gregory et al. \(1989\)](#):

$$(2) {}^{47}R_{\text{measured}} - {}^{47}R_{\text{equilibrium}} = ({}^{47}R_{\text{initial}} - {}^{47}R_{\text{equilibrium}}) e^{-k_{47}t}$$

where in this equation, the 'measured' value has been modified from the initial value after time 't'. Consequently,

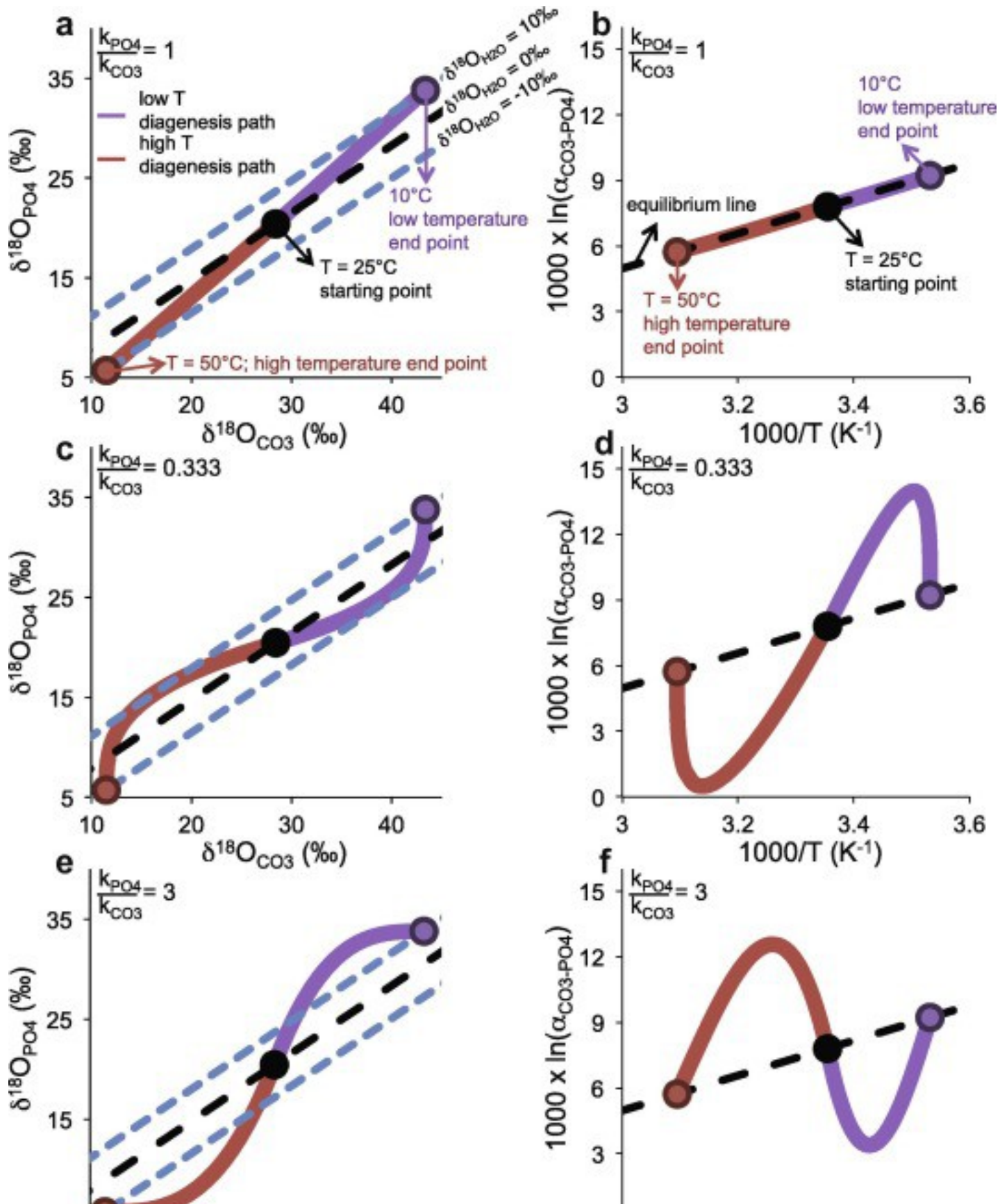
$$(3) F_{47} = (F_{CO3}) k_{47} / k_{CO3}$$

where  $F_{47} = ({}^{47}R_{\text{measured}} - {}^{47}R_{\text{equilibrium}}) / ({}^{47}R_{\text{initial}} - {}^{47}R_{\text{equilibrium}})$  and  $k_{47}$  is the rate constant. Equations similar to (2) have been derived for or applied to other clumped-isotope studies

involving kinetic processes ([Passey and Henkes, 2012](#), [Affek, 2013](#), [Clog et al., 2015](#)). Because  $\Delta_{47}$  values depend not only on  $^{47}\text{R}$  values, but also on bulk isotopic composition, the full equation describing the change in  $\Delta_{47}$  with time is:

$$\Delta_{47} = (\Delta_{47}^{\text{initial}} - \Delta_{47}^{\text{equilibrium}}) \times \left( \frac{k_{47}}{k_{\text{CO}_3} + \Delta_{47}^{\text{equilibrium}}} \right) \times \left( \frac{1}{1 + \frac{13\text{R} \times 18\text{R} + 13\text{R} \times (17\text{R})^2 + 217\text{R} \times 18\text{R}}{1 \times 1000}} \right)$$

where the denominator is equivalent to  $^{47}\text{R}^*$  ([Affek and Eiler, 2006](#)). For all calculations we hold the  $\delta^{13}\text{C}$  value of the carbonate groups constant. We note that large differences in both the  $\delta^{13}\text{C}$  and  $\delta^{18}\text{O}$  (e.g., 10‰) of the starting and ending carbonate compositions can cause non-linear clumped-isotope mixing effects (e.g., [Eiler and Schauble, 2004](#)) that are large enough to be worth considering. For example, take two carbonate minerals with identical  $\Delta_{47}$  values and let one have  $\delta^{18}\text{O}$  and  $\delta^{13}\text{C}$  values 10‰ lower than the other. An equal mixture of the two will have a  $\Delta_{47}$  value  $\sim 0.025\%$  higher than either of the end members. We avoid this complexity here by fixing  $\delta^{13}\text{C}$ , which greatly diminishes this [non-linearity](#), introducing deviations of  $< 0.001\%$  from linear mixing of  $\Delta_{47}$ . In order to calculate the oxygen isotopic composition of apatite phosphate and carbonate groups in isotopic equilibrium with water we used the fractionation factors of [Kolodny et al. \(1983\)](#) and [Lécuyer et al. \(2010\)](#). We do not use the [Shemesh et al. \(1988\)](#) calibration due to its dependence on high temperature ( $> 300\text{ }^\circ\text{C}$ ) points that are either poorly constrained or imply a crossover (which may be present, but in any case prohibits linear interpolations; see above). We used the [Lécuyer et al. \(2010\)](#) over the [Kim and O'Neil \(1997\)](#) calibration because the [Lécuyer et al. \(2010\)](#) calibration was experimentally generated with carbonate groups in apatites (though hydroxyapatites) as opposed to [calcites](#). We acknowledge, though, that these calibrations may, themselves, be inaccurate, but consider them the best currently available for this model. To aid in understanding this model, we provide a schematic figure ([Fig. 6](#)) that illustrates the different paths that diagenesis takes in the composition spaces of [Figs. 3](#) and [5](#) depending on the temperature at which the diagenesis occurs as well as the ratio of  $k_{\text{PO}_4}/k_{\text{CO}_3}$ .



1. [Download high-res image \(622KB\)](#)
2. [Download full-size image](#)

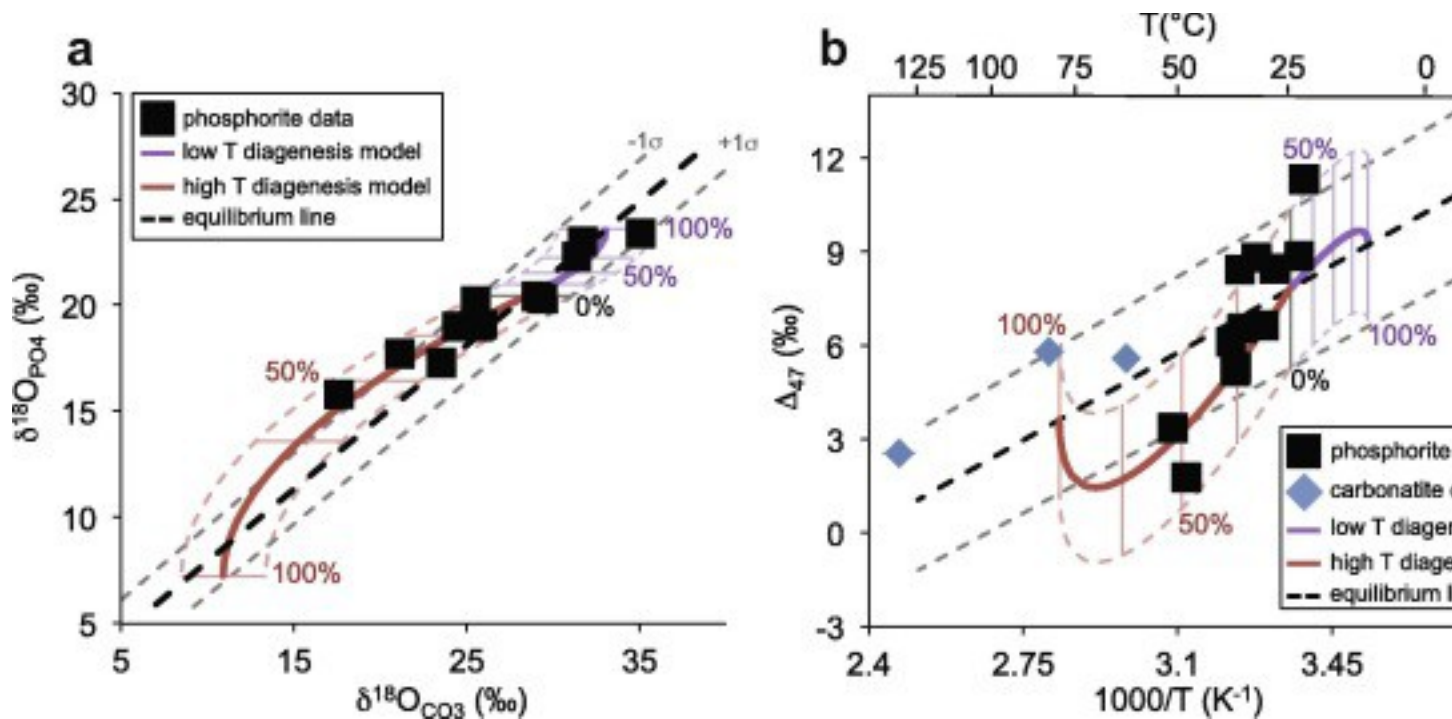
Fig. 6. Schematic figure showing the diagenetic paths that [oxygen-isotope](#) exchange of phosphate and [carbonate groups](#) in [apatite](#) with water take in the spaces outlined in [Figs. 3](#) and [5](#). The legend is given in (a). Dotted lines represent lines of isotopic equilibrium between carbonate and [phosphate groups](#) and clumped-isotope equilibrium. Solid lines are the diagenetic paths. In red is the high-temperature diagenetic path and in purple the low-temperature diagenetic path. The black circle represents the starting composition and the red and purple circles the ending composition for the high- and low-temperature paths respectively. In (a) and (b), phosphate and carbonate groups exchange [oxygen isotopes](#) with water at an equal rate. In (c) and (d), carbonate groups exchange oxygen isotopes with water more quickly than phosphate groups do. In (e) and (f), phosphate exchange oxygen isotopes more quickly with water than carbonate groups do. In all cases  $k_{47}/k_{CO3} = 1$  and  $\delta^{13}CCO3$  is held constant. (For interpretation of the references to color in this figure legend, the reader is referred to the web version of this article.)

## 5.2. Application of the model to conditions relevant for phosphorite formation and diagenesis

We applied this model to [phosphorite](#) formation and modification in the context of bulk and clumped isotopic compositions for two different diagenetic paths. For both, we assumed that all samples initially formed in oxygen and clumped-isotope equilibrium at 25 °C in water with a  $\delta^{18}O$  value of 0‰ (the approximate average value of seawater today). This is clearly an oversimplification, but we consider it sufficient for the exploration of the model as a valid framework to describe the data. The first pathway has diagenesis occurring at 80 °C (i.e., hotter than initial formation temperatures) in pore waters with  $\delta^{18}O = -4‰$ . Such environments commonly occur ~1.5 to 3 km oceanic sediments sitting on [oceanic crust](#) with geotherms ranging from 20 to 40 °C/km and decreases in pore-water  $\delta^{18}O$  of ~2–15‰/km ([Lawrence and Gieskes, 1981](#)). Alternatively, such low  $\delta^{18}O$  pore waters could also result from infiltration of [meteoric waters](#) ([Epstein and Mayeda, 1953](#), [Craig, 1961](#), [Dansgaard, 1964](#), [Bowen, 2010](#)) into sediments. The second pathway is modeled to occur at 10 °C (i.e. colder than the initial formation temperature) in waters that are isotopically identical to the [formation waters](#) ( $\delta^{18}O = 0‰$ ). Such a scenario could be imagined to occur if sinking bones and teeth (e.g., from fish) or continentally derived apatites were deposited and underwent reaction in cold, deep waters on a [continental slope](#). It is worth noting that these paths



are not mutually exclusive — materials may first undergo diagenetic reactions during deposition in cold water followed by diagenesis at elevated temperatures. These models require a choice for both the ratio of  $k_{47}/k_{CO3}$  and  $k_{PO4}/k_{CO3}$ . We chose  $k_{47}/k_{CO3}$  to be equal to 1, implying no difference in  $^{18}O/^{16}O$  [exchange rate](#) on  $^{13}C$  abundance. This assumption is consistent with experimental results constraining rates of exchange between  $CO_2$  and liquid water ([Affek, 2013](#), [Clog et al., 2015](#)). We used a value of 1 because it is the expected value if carbonate ions in solution are always in both oxygen-isotope equilibrium with water and clumped-isotope equilibrium. In this case, the rate of isotopic exchange between mineral and water should be governed only by the net rate of dissolution and reprecipitation reactions. We chose the  $k_{PO4}/k_{CO3}$  value that simultaneously best fit the data (using a least-squares minimization) in both [Fig. 3a](#) and b, and along both diagenetic pathways ([Fig. 7](#)). This yielded a value of 0.53. However, we note that visually acceptable fits range from 0.3 to 0.6. This ratio could and should vary across environments depending on, for example, inorganic dissolution and reprecipitation rates, mineral composition, availability of organisms to enzymatically catalyze oxygen exchange in  $PO_4^{3-}$  groups, and temperature. For simplicity and in the absence of better constraints, we have chosen a constant value for the model. We note that this value is distinct from those found by [Zazzo et al. \(2004\)](#) for experimental dissolution and reprecipitation of fossil [hydroxyapatite](#) in the presence of microorganisms ( $k_{PO4}/k_{CO3}$  from 2 to 15) as discussed above and is more similar to the ratio of 0.1 obtained for the inorganic experiments. This may indicate that inorganic reactions are significant during phosphate oxygen-isotope-exchange processes during diagenesis.



1. [Download high-res image \(281KB\)](#)
2. [Download full-size image](#)

Fig. 7. Comparison of data to modeled trajectories during [diagenesis](#). The model is described and developed in the text (Section 5). All samples are assumed to have precipitated in isotopic equilibrium at 25 °C in waters with a  $\delta^{18}\text{O}$  value of 0‰. Diagenesis at higher temperatures is assumed to occur at 80 °C in waters with a  $\delta^{18}\text{O}$  value of -4‰. Diagenesis at cooler temperatures is assumed to occur at 10 °C in waters with a  $\delta^{18}\text{O}$  value of 0‰. The amount of diagenesis relative to the final value is given by the percentages with gradations of 25%. The best-fit value for  $k_{\text{PO}_4}/k_{\text{CO}_3}$  was found to be 0.53 (see text). (a) Comparison of bulk  $\delta^{18}\text{O}_{\text{CO}_3}$  and  $\delta^{18}\text{O}_{\text{PO}_4}$  values vs. the model. (b) Comparison of  $1000 \times \ln(\alpha_{\text{CO}_3\text{-PO}_4})$  vs.  $1000/T$  where  $T$ , in Kelvin, is the derived clumped-isotope-based temperature vs. the model. [Carbonatite](#)  $\delta^{18}\text{O}_{\text{CO}_3}$  and clumped-isotope-based temperatures come from [Stolper and Eiler \(2015\)](#) for the Siilinjarvi and Oka apatites. The  $\delta^{18}\text{O}_{\text{PO}_4}$  value for Siilinjarvi apatites was taken to be 4.9‰ using data from [Tichomirowa et al. \(2006\)](#). The  $\delta^{18}\text{O}_{\text{PO}_4}$  value for Oka apatites was taken to be 5.6‰ using data from [Conway and Taylor, Jr \(1969\)](#).  $1\sigma$  error ranges given for the model in the lighter colored, thinner lines were derived using the errors estimates given for the published  $\text{PO}_4\text{-H}_2\text{O}$  [oxygen-isotope fractionation](#) factor given in [Lécuyer et al. \(2010\)](#) and propagating that error through the model. Error bars describing the analytical precision of the measurements are smaller than the data points. (For interpretation of the references to colour in this figure legend, the reader is referred to the web version of this article.)

### 5.3. Comparison of the model framework to the data

We provide the calculated model trajectories for this diagenetic framework in [Fig. 7](#). A few key insights can be taken away from this exercise. First, as seen in [Fig. 7](#), this diagenetic model is able to capture the overall structure of the measured data for both the bulk isotopes and clumped isotopes. This indicates the bulk and clumped-isotope compositions of phosphorites can be explained, to first order, by formation in isotopic equilibrium with water and then, for altered samples, diagenesis at either elevated temperatures in waters with lower  $\delta^{18}\text{O}$  values or diagenesis at lower temperatures in waters of similar isotopic composition as formation. The overall success of the model at describing the trends in the data indicates that the combination of  $\delta^{18}\text{OPO}_4$ ,  $\delta^{18}\text{OCO}_3$ , and temperatures based on  $\Delta_{47}$  values provide a more complete understanding of both the formation and subsequent modification of these samples.

Despite this success, the model is clearly only suitable, as applied, here, for first-order conclusions. For example, samples scatter about the trends and, especially for the low temperature paths, do not yield precisely the same amount of diagenesis in both [Figs. 7a](#) and [b](#). Some of this disagreement is likely related to our assumption that all phosphorites form at identical temperatures and in fluids with identical  $\delta^{18}\text{O}$  values and then undergo diagenesis along one of two paths with fixed temperatures, relative rate constants, and  $\delta^{18}\text{O}_{\text{H}_2\text{O}}$  values. This is clearly a gross oversimplification. Finally, it is not clear that the chosen fractionation factors for oxygen isotope equilibrium between carbonate and phosphate groups in apatite are correct. Presumably the scatter in the data about the trajectories of the model is related, at least in part, to mismatches between the data and the simplicity of our model assumptions. Nevertheless, the [critical point](#) is that the main trend in the data is consistent with a simple, plausible model of diagenesis.

Second, the comparison of the diagenetic model to the data provides a potential insight into the creation and diagenesis of phosphorites (and perhaps other carbonate bearing materials) with  $\delta^{18}\text{O}$  values that are several per mil lower than is commonly observed in modern day marine phosphates. Such low  $\delta^{18}\text{O}$  values are often assumed to be the result of diagenesis in meteorically derived fluids or in marine pore waters at elevated temperatures (e.g., [Degens and Epstein, 1962](#), [Killingley, 1983](#), [Land, 1995](#)). However, there are alternative explanations for low  $\delta^{18}\text{O}$  values in ancient samples that instead invoke a change in the  $\delta^{18}\text{O}$  value of the ocean to lower values (e.g., [Veizer et al., 1997](#), [Veizer et al., 1999](#), [Kasting et al., 2006](#), [Jaffrés et al., 2007](#)) or precipitation of samples in the past at elevated temperatures (e.g., [Knauth and Epstein, 1976](#), [Karhu](#)

[and Epstein, 1986](#)). The association we observe between higher clumped-isotope temperatures and lower  $\delta^{18}\text{O}$  values ([Figs. 3](#) and [5](#)), combined with the fit of the model to the data, is most consistent with the interpretation that diagenesis plays a key role in lowering the  $\delta^{18}\text{O}$  value of many phosphorites.

Third, the success of the model supports the view that  $\text{PO}_4^{3-}$  groups are more resistant to exchange in [natural materials](#) than  $\text{CO}_3^{2-}$  groups ([Shemesh et al., 1983](#), [Shemesh et al., 1988](#), [Longinelli et al., 2003](#)). However, it is also clear from this data that in the case of phosphorites, apatites can be open to significant amounts of oxygen-isotope exchange with water for both carbonate and phosphate groups. Indeed, the arrays observed in [Fig. 7](#) could potentially be used as a test of diagenesis in other samples — if samples fall on [disequilibrium](#) arrays in both the  $\delta^{18}\text{OCO}_3$ – $\delta^{18}\text{OPO}_4$  space ([Fig. 7a](#)) and  $\Delta_{47}$ -based temperature space ([Fig. 7b](#)) the presence of diagenesis could be identified unambiguously.

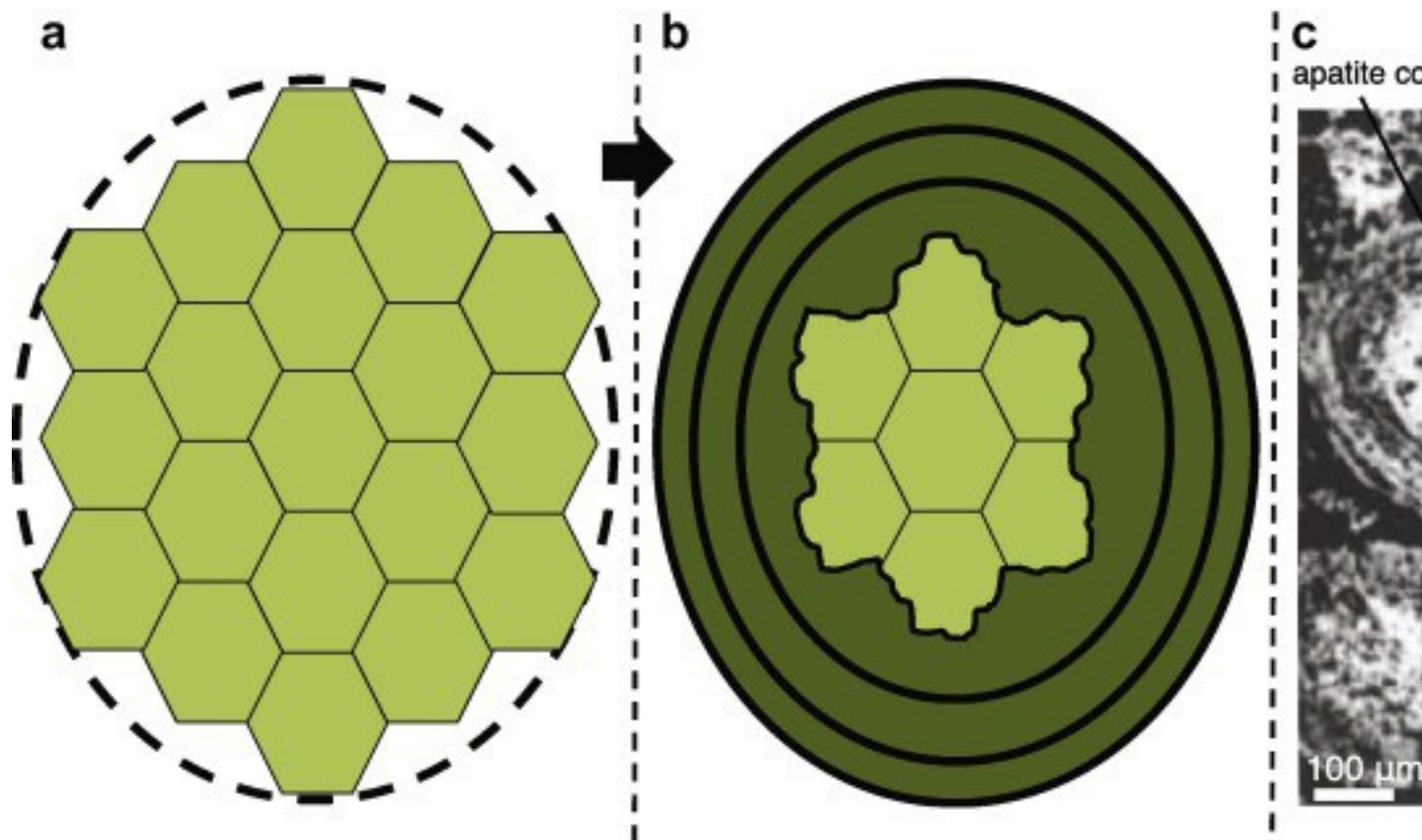
## 6. Do apatites ever fully re-equilibrate their oxygen isotopes during diagenesis?

An interesting aspect of the model when fit to the data is that for the high-temperature [diagenesis](#) pathway, no samples appear to return to the lines that define oxygen and internal isotopic equilibrium in [Fig. 5a](#) and [b](#). Instead, all samples observed remain below  $\sim 50\%$  re-equilibration ([Fig. 7](#)). The precise percent of re-equilibration is controlled by the assumed temperature of the diagenetic reactions. Thus our finding of 50% is qualitative. What is important is that no samples with elevated clumped-isotope temperatures or low  $\delta^{18}\text{OCO}_3$  or  $\delta^{18}\text{OPO}_4$  values have returned to the values expected for an isotopically equilibrated mineral.

A question then is do apatites, once isotopically modified, ever return to isotopic equilibrium both internally for clumped isotopes and for [oxygen-isotope](#) equilibrium between phosphate and [carbonate groups](#)? To answer this, we compared the [phosphorite apatite](#) samples to apatites from igneous [carbonatite](#) intrusions that formed at elevated temperatures. These igneous apatites crystallized at temperatures above  $\sim 600$  °C or so, but preserve lower clumped-isotope temperatures due to internal isotope-exchange reactions that take place during cooling ([Stolper and Eiler, 2015](#)). Thus, their clumped-isotope compositions are altered after mineral [crystallization](#), but in a different process from the phosphorites. In contrast to the phosphorites, these igneous samples fall on or near the expected range of [equilibrium lines](#) (within the  $\pm 1\sigma$  error bounds) for their clumped-isotope temperature ([Fig. 7b](#); we do not include them in [7a](#) as this space depends on the [isotopic composition](#) of [formation waters](#) which is not relevant

for igneous apatites). This analysis indicates that during cooling, when these exchange reactions ceased, the clumped-isotope and oxygen-isotope compositions of the  $\text{PO}_4^{3-}$  and  $\text{CO}_3^{2-}$  groups 'closed' at the same temperature. Thus, apatites that undergo reactions that alter their carbonate and phosphate oxygen-isotope and clumped-isotope compositions after formation can end up in or near the positions expected for isotopic equilibrium in Figs. [3b](#), [5b](#) and [7b](#). This finding may have implications for our understanding of the [chemical controls](#) of the clumped-isotope apparent blocking temperature in apatite — i.e., internal resetting in apatites likely depends on exchange of an [oxygen atom](#) between a phosphate and carbonate ion group.

Based on this, we must now ask why it is that the diagenetically modified phosphorites, even those hundreds of millions of years old, have not fully re-equilibrated their [oxygen isotopes](#) between carbonate and phosphate groups? From the data and model, it appears that apatites readily undergo 10's of percent re-equilibration towards diagenetic conditions, but struggle to go to completion. The answer to this may lie with the fact that the model of [Criss et al. \(1987\)](#) and [Gregory et al. \(1989\)](#) implicitly assumes that all oxygen bearing groups are equally capable of undergoing isotope-exchange reactions at all times. However in nature this is not necessarily the case. For example, water may be incapable of penetrating and exchanging oxygen with all atoms in an apatite grain due to a lack of pores/channels to the interior of the original mineral. We suggest that this occurs due to 'armoring' of original grains with impermeable diagenetic rims as schematically outlined and shown with natural samples in [Fig. 8](#). Indeed the presence of apatite cores surrounded and armored with apatite rims is commonly observed in phosphorite deposits ([Fig. 8](#); [Cook, 1972](#), [Braithwaite, 1980](#), [Glenn and Arthur, 1988](#)).



1. [Download high-res image \(431KB\)](#)
2. [Download full-size image](#)

Fig. 8. Cartoon representation of the [diagenesis](#) of an [apatite](#) grain in comparison to grains from a [phosphorite](#) deposit. (a) Starting collection of apatite minerals. (b) Dissolution and reprecipitation of these minerals arms an inner, original core with an outer rim of diagenetic apatite. This outer rim would prevent further diagenesis of the [inner core](#). (c) [Photomicrograph](#) of phosphorite apatites from the Peru margin. Displayed are apatite ooids (Od) with an apatite core (as marked) and concentric layers of apatite rimming the core (as marked). The photomicrograph was modified from [Fig. 6b](#) of [Glenn and Arthur \(1988\)](#). Reprinted with permission from Elsevier. The importance of such geometric restrictions on the rates of dissolution and reprecipitation has recently been modeled quantitatively and shown to be of generic importance to minerals undergoing diagenesis ([Reeves and Rothman, 2013](#)). If correct, such a model indicates that the temperatures derived from clumped-isotope analyses of mixtures of relict and newly grown minerals, even those heavily modified by diagenesis, do not represent any particular diagenetic [recrystallization](#) temperature or event. The temperatures instead represent a mixed signal originating from both the original depositional temperature and the temperature range over which diagenesis occurred. If

this phenomenon occurs elsewhere, e.g., in [calcites](#) or [dolomites](#), it may have implications for the meaning of clumped-isotope based reconstructions of diagenetic recrystallization temperatures and [fluid compositions](#). This model could be tested by using an [ion probe](#) to measure the difference in  $\delta^{18}\text{O}$  between phosphate cores vs. rims. This is because the model presented above predicts significant (5–10‰) differences in  $\delta^{18}\text{O}$  values between the relict, original core and the rim that formed during diagenesis. If the model is correct, it would indicate that clumped-isotope temperatures of bulk, diagenetically altered phosphorites (and perhaps other carbonate-bearing phases) do not represent a discrete temperature of diagenesis, as has been assumed, but instead represent the integrated history of formation and alteration, incorporating signals from both original precipitation and later diagenetic modification at a variety of temperatures.

## 7. Summary and conclusions

The measurements of [oxygen isotopes](#) of [carbonate groups](#) and [phosphate groups](#) in apatites from [phosphorites](#) combined with clumped-isotope temperatures for the carbonate groups yield linear relationships between  $\delta^{18}\text{OCO}_3$  and  $\delta^{18}\text{OPO}_4$  as well as  $1000\ln(\alpha_{\text{CO}_3\text{-PO}_4})$  and  $1/T$  where  $T$  is the derived clumped-isotope temperature of the carbonate groups. These relationships cannot be fully reconciled with any current equilibrium-based interpretation of the bulk isotopes or clumped-isotope temperatures. Instead, the clumped-isotope temperatures of phosphorites demonstrate and reinforce that isotopic equilibrium captured during mineral formation is overprinted by diagenetic reactions in many samples. We interpreted and modeled these results in a quantitative framework that incorporates isotope-exchange reactions during [diagenesis](#). In this model, the originally precipitated samples exchange oxygen isotopes with water during diagenesis. Using this model, we showed the relationships observed between  $\delta^{18}\text{OCO}_3$ ,  $\delta^{18}\text{OPO}_4$ , and the clumped-isotope temperatures can be understood as the consequence of varying amounts of [oxygen-isotope](#) exchange for both phosphate and carbonate groups with fluids. We required that the isotope-exchange reactions occur at different temperatures and fluid [isotopic compositions](#) as compared to the original formation, with most altered samples best fit by diagenesis in a higher temperature setting with lower  $\delta^{18}\text{O}$  fluids. Furthermore this kinetic framework required more rapid isotope exchange reactions between carbonate and water vs. phosphate and water. This supports the hypothesis that apatites in phosphorites undergo isotopic exchange reactions with water in both the carbonate and phosphate groups during burial and diagenesis, but that the phosphate groups are more resilient to modification than the carbonate groups. This model indicates that for phosphorites that have been isotopically

modified, both elevated temperatures and waters with  $\delta^{18}\text{O}$  values lower than seawater are involved. Such information provides insight into the timing and location of diagenesis suggesting that diagenetic isotope-exchange reactions occur during burial at kilometer depths in fluids that are only slightly modified from seawater.

An additional insight from the model is that none of the sedimentary phosphorites, even those hundreds of millions of years old, re-established isotopic equilibrium during diagenesis; i.e., the carbonate and phosphate groups never developed an oxygen-isotope [fractionation](#) consistent with the diagenetic temperature implied by the clumped-isotope compositions of carbonate groups. This lack of full isotopic re-equilibration is interpreted as a consequence of the fact that phosphorite diagenesis leads to armoring of relict primary [apatite](#) with rims of secondary diagenetic apatite, preventing further diagenesis of the relict cores. In instances such as this, the clumped-isotope temperatures of bulk diagenetically modified phases reflect mixing between apatite formed at the original mineral formation temperature and secondary apatite formed at a range of diagenetic reaction temperatures. This insight may have implications for the interpretation clumped-isotope temperatures of diagenetically modified phases in other settings and minerals.

## Acknowledgements

We wish to thank Yehoshua Kolodny and Boaz Luz of the Hebrew University in Jerusalem for providing the samples and helpful discussions. We additionally wish to thank Aldo Shemesh of the Weizmann Institute for helpful discussions. We thank two anonymous reviewers, Cedric John, and our associate editor, Hagit Affek, for helpful comments. DAS would like to thank his PhD thesis committee of Jess Adkins, Woodward Fischer, John Grotzinger, and Alex Sessions (along with John Eiler) for sage advice and guidance. DAS acknowledges the NSF GRFP for support. JME acknowledges the support of the NSF-EAR program for instrumentation.

## Appendix A

A1. A recalculation of the dependence of  $\Delta_{47}$  in the absolute reference frame on temperature taking into account the acid digestion correction used in this study. We modified the translation of the [Ghosh et al. \(2006\)](#) calibration to absolute reference frame as given in [Dennis et al. \(2011\)](#) to take into account new results on the value of the [acid digestion fractionation](#) factor between 90 °C and 25 °C acid baths in the absolute reference frame. Specifically, [Henkes et al. \(2013\)](#) demonstrated that the difference between samples prepared using 90 °C and 25 °C acid baths is, on average, 0.092‰ ( $\pm 0.007$ , 1 s.e.) in the absolute reference frame, and thus higher than the acid



digestion factor (0.081‰) used in [Dennis et al. \(2011\)](#) to convert all measurements to a 25 °C reference frame. We note that there have been recent suggestions for other values for this acid-digestion fractionation factor in the absolute reference frame including 0.066‰ for [aragonite](#) and 0.075‰ for [calcite](#) ([Wacker et al., 2013](#)) and 0.082‰ for calcite, aragonite, and [dolomite](#) ([Defliese et al., 2015](#)). Use of these different fractionation factors would change temperatures by up to ~6 °C at the temperature interval of interest to this study (20–50 °C). We chose to use the [Henkes et al. \(2013\)](#) calibration as the CO<sub>2</sub> extraction line used in that studied was modeled after that used at Caltech. When this value (0.092‰) is used to place the NBS 19 standard measured in both the [Ghosh et al. \(2006\)](#) and [Dennis et al. \(2011\)](#) studies into the absolute reference frame, the value becomes 0.400‰ as opposed to 0.392‰, as calculated in [Dennis et al. \(2011\)](#). Repeating the calculations performed in [Dennis et al. \(2011\)](#) to convert the  $\Delta_{47}$ -values of [Ghosh et al. \(2006\)](#) into the absolute reference, but using this new value for NBS 19 for the correction results in the following equation describing the dependence of  $\Delta_{47}$  on temperature:

$$(A1)\Delta_{47}=0.0636\times 106T-0.006$$

We note that this change in the equation, though more accurate, is relatively unimportant — differences between using the equation provided in [Dennis et al. \(2011\)](#) and Eq. (A1) result in differences in temperature of less than 0.2 °C between the calibrations from 1 to 50 °C, the range of temperatures used in the calibration.

Table A1.  $\Delta_{47}$  accuracy and precision of standards and [phosphorite](#) samples.

	$n^a$	$\Delta_{47,ARF, \text{this study}} (\text{‰})^b$	$\pm^c$	$\Delta_{47, \text{Caltech}} (\text{‰})^{b,d}$	$\Delta_{47, \text{Dennis et al. (2011)}} (\text{‰})^{b,e}$
Carrara Marble	36	0.399	0.017	0.401	0.403
TV01	31	0.721	0.013	0.724	–
Average					–
Phosphorites <sup>f</sup>	69	–	0.021	–	–

a

Number of samples measured.

b

Given in the absolute reference frame (ARF) of [Dennis et al. \(2011\)](#).

c

1 standard deviation.

d

Average, long-term value at Caltech.

e

This value (in the absolute reference frame) is derived from [Dennis et al. \(2011\)](#) by taking the average value for the reported Carrara in-house marbles and increasing the Harvard, Johns Hopkins, and Caltech values by 0.011‰ to account for the use of a 90 °C clumped isotope acid digestion fractionation of 0.092‰ used in this study instead of 0.081‰ as was used in that study.

f

Only the standard deviation for the precision of all phosphorite measurements is given. This was done by taking the difference of each sample's  $\Delta_{47}$  from the average value of the replicates for all samples and then taking the standard deviation of those differences for all data. No average is given as all samples are used for this analysis.

Table A2.  $\delta^{13}\text{C}$  and  $\delta^{18}\text{O}$  accuracy and precision of standards and [phosphorite](#) samples.

	$n^a$	$\delta^{18}\text{O}_{\text{this study}}(\text{‰})^b$	$\pm^c$	$\delta^{18}\text{O}_{\text{Caltech}}(\text{‰})^{b,d}$	$\delta^{13}\text{C}_{\text{this study}}(\text{‰})^e$	$\pm^c$	$\delta^{13}\text{C}_{\text{Caltech}}(\text{‰})^{d,e}$
Carrara marble	36	28.87	0.07	28.83	2.35	0.02	2.32
TV01	31	22.05	0.10	22.03	2.55	0.05	2.53
Average							
Phosphorites <sup>f</sup>	69	–	0.24	–	–	0.05	–

a

Number of samples measured.

b

Referenced to VSMOW.

c

1 standard deviation.

d

Average, long-term value at Caltech.

e

Referenced to the VPDB scale.

f

Only the standard deviation for the precision of all phosphorite measurements is given. This was done by taking the difference of each sample's  $\delta$  from the average value of the replicates for all samples and then taking the standard deviation of those differences for all data. No average is given as all samples are used for this analysis.

## Appendix B. Supplementary data

[Download spreadsheet \(49KB\)](#)[Help with xlsx files](#)

Supplementary data.

## References

### [Affek and Eiler, 2006](#)

H.P. Affek, J.M. Eiler **Abundance of mass 47 CO<sub>2</sub> in urban air, car exhaust, and human breath**  
Geochim. Cosmochim. Acta, 70 (2006), pp. 1-12

[Article](#)[Download PDF](#)[View Record in Scopus](#)

### [Affek et al., 2008](#)

H.P. Affek, M. Bar-Matthews, A. Ayalon, A. Matthews, J.M. Eiler **Glacial/interglacial temperature variations in Soreq cave speleothems as recorded by 'clumped isotope' thermometry**  
Geochim. Cosmochim. Acta, 72 (2008), pp. 5351-5360

[Article](#)[Download PDF](#)[View Record in Scopus](#)

### [Affek, 2013](#)

H.P. Affek **Clumped isotopic equilibrium and the rate of isotope exchange between CO<sub>2</sub> and water**

Am. J. Sci., 313 (2013), pp. 309-325

[CrossRef](#)[View Record in Scopus](#)

### [Ayliffe et al., 1992](#)

L.K. Ayliffe, H. Herbert Veeh, A.R. Chivas **Oxygen isotopes of phosphate and the origin of island apatite deposits**

Earth Planet. Sci. Lett., 108 (1992), pp. 119-129

[Article](#)[Download PDF](#)[View Record in Scopus](#)

### [Ayliffe et al., 1994](#)

L. Ayliffe, A. Chivas, M. Leakey **The retention of primary oxygen isotope compositions of fossil elephant skeletal phosphate**

Geochim. Cosmochim. Acta, 58 (1994), pp. 5291-5298

[Article](#)[Download PDF](#)[View Record in Scopus](#)

### [Baioumy et al., 2007](#)

H. Baioumy, R. Tada, M. Gharaié **Geochemistry of Late Cretaceous phosphorites in Egypt: implication for their genesis and diagenesis**

J. Afr. Earth Sci., 49 (2007), pp. 12-28

[Article](#)[Download PDF](#)[View Record in Scopus](#)

### [Birch et al., 1983](#)

G. Birch, J. Thomson, J. McArthur, W. Burnett **Pleistocene phosphorites off the west coast of South Africa**

Nature, 302 (1983), pp. 601-603

[CrossRef](#)[View Record in Scopus](#)

[Blake et al., 1997](#)

R.E. Blake, J. O'Neil, G. Garcia **Oxygen isotope systematics of biologically mediated reactions of phosphate: I. Microbial degradation of organophosphorus compounds**  
Geochim. Cosmochim. Acta, 61 (1997), pp. 4411-4422

[ArticleDownload PDFView Record in Scopus](#)

[Bowen, 2010](#)

G.J. Bowen **Isoscapes: spatial pattern in isotopic biogeochemistry**  
Annu. Rev. Earth Planet. Sci., 38 (2010), pp. 161-187

[CrossRefView Record in Scopus](#)

[Bradbury et al., 2015](#)

H.J. Bradbury, V. Vandeginste, C.M. John **Diagenesis of phosphatic hardgrounds in the Monterey Formation: a perspective from bulk and clumped isotope geochemistry**  
Geol. Soc. Am. Bull., B31160 (2015), p. 31161

[Braithwaite, 1980](#)

C.J. Braithwaite **The petrology of oolitic phosphorites from Esprit (Aldabra), western Indian Ocean**

Philos. Trans. Royal Soc. Lond. Series B, Biol. Sci. (1980), pp. 511-540

[CrossRef](#)

[Bremner and](#)

[Rogers, 1990](#)

J. Bremner, J. Rogers **Phosphorite deposits on the Namibian continental shelf**  
Phosphate Deposits of the World, 3 (1990), pp. 143-152

[View Record in Scopus](#)

[Came](#)

[et al.,](#)

[2007](#)

R.E. Came, J.M. Eiler, J. Veizer, K. Azmy, U. Brand, C.R. Weidman **Coupling of surface temperatures and atmospheric CO<sub>2</sub> concentrations during the Palaeozoic era**

Nature, 449 (2007), pp. 198-201

[CrossRefView Record in Scopus](#)

[C  
I  
o  
g  
-  
e  
t  
-  
a  
!](#)

M. Clog, D. Stolper, J.M. Eiler **Kinetics of CO<sub>2(g)</sub>-H<sub>2</sub>O<sub>(l)</sub> isotopic exchange, including mass 47 isotopologues**

Chem. Geol., 395 (2015), pp. 1-10

[ArticleDownload](#) [PDFView](#) [Record in Scopus](#)

[Conway](#)  
[and](#)  
[Taylor,](#)  
[1969](#)

C.M. Conway, H.P. Taylor Jr **O<sup>18</sup>/O<sup>16</sup> and C<sup>13</sup>/C<sup>12</sup> ratios of coexisting minerals in the Oka and Magnet Cove carbonatite bodies**

J. Geol. (1969), pp. 618-626

[CrossRefView](#) [Record in Scopus](#)

[Cook, 1972](#)

P.J. Cook **Petrology and geochemistry of the phosphate deposits of northwest Queensland, Australia**

Econ. Geol., 67 (1972), pp. 1193-1213

[CrossRefView](#) [Record in Scopus](#)

[Craig, 1961](#)

H. Craig **Isotopic variations in meteoric waters**

Science, 133 (1961), pp. 1702-1703

[View Record in Scopus](#)

[Criss et al., 1987](#)

R. Criss, R. Gregory, H. Taylor Jr **Kinetic theory of oxygen isotopic exchange between minerals and water**

Geochim. Cosmochim. Acta, 51 (1987), pp. 1099-1108

[ArticleDownload](#) [PDFView](#) [Record in Scopus](#)

[Daëron et al., 20](#)

M. Daëron, W. Guo, J. Eiler, D. Genty, D. Blamart, R. Boch, R. Drysdale, R. Maire, K. Wainer, G. Zanchetta **<sup>13</sup>C/<sup>18</sup>O clumping in speleothems: Observations from natural caves and precipitation experiments**

Geochim. Cosmochim. Acta, 75 (2011), pp. 3303-3317

[ArticleDownload](#) [PDFView](#) [Record in Scopus](#)

[Dansgaard, 1964](#)

W. Dansgaard **Stable isotopes in precipitation**

Tellus, 16 (1964), pp. 436-468

[CrossRefView Record in Scopus](#)

[Defliese et al., 2015](#)

W.F. Defliese, M.T. Hren, K.C. Lohmann **Compositional and temperature effects of phosphoric acid fractionation on  $\Delta_{47}$  analysis and implications for discrepant calibrations**

Chem. Geol. (2015)

[Degens and Epstein, 1962](#)

E.T. Degens, S. Epstein **Relationship between  $O^{18}/O^{16}$  ratios in coexisting carbonates, cherts, and diatomites: geological notes**

AAPG Bull., 46 (1962), pp. 534-542

[View Record in Scopus](#)

[Dennis and Schrag, 2010](#)

K.J. Dennis, D.P. Schrag **Clumped isotope thermometry of carbonatites as an indicator of diagenetic alteration**

Geochim. Cosmochim. Acta, 74 (2010), pp. 4110-4122

[ArticleDownload PDFView Record in Scopus](#)

[Dennis et al., 2011](#)

K.J. Dennis, H.P. Affek, B.H. Passey, D.P. Schrag, J.M. Eiler **Defining an absolute reference frame for 'clumped' isotope studies of  $CO_2$**

Geochim. Cosmochim. Acta, 75 (2011), pp. 7117-7131

[ArticleDownload PDFView Record in Scopus](#)

[Eagle et al., 2010](#)

R.A. Eagle, E.A. Schauble, A.K. Tripathi, T. Tütken, R.C. Hulbert, J.M. Eiler **Body temperatures of modern and extinct vertebrates from  $^{13}C-^{18}O$  bond abundances in bioapatite**

Proc. Natl. Acad. Sci., 107 (2010), p. 10377

[CrossRefView Record in Scopus](#)

[Eagle et al., 2011](#)

R.A. Eagle, T. Tütken, T.S. Martin, A.K. Tripathi, H.C. Fricke, M. Connely, R.L. Cifelli, J.M. Eiler **Dinosaur body temperatures determined from isotopic ( $^{13}C-^{18}O$ ) ordering in fossil biominerals**

Science, 333 (2011), p. 443

[CrossRefView Record in Scopus](#)

[Eagle et al., 2013](#)

Eagle R., Eiler J. M., Tripathi A. K., Ries J., Freitas P., Hiebenthal C., Wanamaker A., Taviani M., Elliot M., Marensi S. (2013) The influence of temperature and seawater carbonate saturation state on  $^{13}C-^{18}O$  bond ordering in bivalve mollusks.

[Eiler and Schauble, 2013](#)

J.M. Eiler, E. Schauble  **$^{18}O^{13}C^{16}O$  in Earth's atmosphere**

Geochim. Cosmochim. Acta, 68 (2004), pp. 4767-4777

[ArticleDownload](#) [PDFView](#) [Record in Scopus](#)

[Eiler, 2007](#)

J.M. Eiler **“Clumped-isotope” geochemistry – The study of naturally-occurring, multiply-substituted isotopologues**

Earth Planet. Sci. Lett., 262 (2007), pp. 309-327

[ArticleDownload](#) [PDFView](#) [Record in Scopus](#)

[Eiler, 2011](#)

J.M. Eiler **Paleoclimate reconstruction using carbonate clumped isotope thermometry**

Quatern. Sci. Rev., 30 (2011), pp. 3575-3588

[ArticleDownload](#) [PDFView](#) [Record in Scopus](#)

[Eiler, 2013](#)

J.M. Eiler **The isotopic anatomies of molecules and minerals**

Annu. Rev. Earth Planet. Sci., 41 (2013), pp. 411-441

[CrossRefView](#) [Record in Scopus](#)

[Epstein and May](#)

S. Epstein, T. Mayeda **Variation of O<sup>18</sup> content of waters from natural sources**

Geochim. Cosmochim. Acta, 4 (1953), pp. 213-224

[ArticleDownload](#) [PDFView](#) [Record in Scopus](#)

[Epstein et al., 19](#)

S. Epstein, R. Buchsbaum, H.A. Lowenstam, H.C. Urey **Revised carbonate-water isotopic temperature scale**

Geol. Soc. Am. Bull., 64 (1953), pp. 1315-1325

[CrossRef](#)

[Ferry et al., 2011](#)

J.M. Ferry, B.H. Passey, C. Vasconcelos, J.M. Eiler **Formation of dolomite at 40–80 °C in the Latemar carbonate buildup, Dolomites, Italy, from clumped isotope thermometry**

Geology, 39 (2011), pp. 571-574

[CrossRefView](#) [Record in Scopus](#)

[Finnegan et al., 2](#)

S. Finnegan, K. Bergmann, J.M. Eiler, D.S. Jones, D.A. Fike, I. Eisenman, N.C. Hughes, A.K. Tripati, W.W. Fischer **The magnitude and duration of Late Ordovician-Early Silurian glaciation**

Science, 331 (2011), p. 903

[CrossRefView](#) [Record in Scopus](#)

[Gammelsrød et](#)

T. Gammelsrød, C. Bartholomae, D. Boyer, V. Filipe, M. O’Toole **Intrusion of warm surface water along the Angolan-Namibian coast in February–March 1995: the 1995 Benguela Niño**

S. Afr. J. Mar. Sci., 19 (1998), pp. 41-56

[CrossRefView](#) [Record in Scopus](#)

[Ghosh et al., 2006](#)

P. Ghosh, J. Adkins, H. Affek, B. Balta, W. Guo, E.A. Schauble, D. Schrag, J.M. Eiler  **$^{13}\text{C}$ – $^{18}\text{O}$  bonds in carbonate minerals: a new kind of paleothermometer**

Geochim. Cosmochim. Acta, 70 (2006), pp. 1439-1456

[ArticleDownload](#) [PDFView](#) [Record in Scopus](#)

[Glenn and Arthur](#)

C.R. Glenn, M.A. Arthur **Petrology and major element geochemistry of Peru margin phosphorites and associated diagenetic minerals: authigenesis in modern organic-rich sediments**

Mar. Geol., 80 (1988), pp. 231-267

[ArticleDownload](#) [PDFView](#) [Record in Scopus](#)

[Gregory et al., 1989](#)

R.T. Gregory, R.E. Criss, H.P. Taylor Jr **Oxygen isotope exchange kinetics of mineral pairs in closed and open systems: applications to problems of hydrothermal alteration of igneous rocks and Precambrian iron formations**

Chem. Geol., 75 (1989), pp. 1-42

[ArticleDownload](#) [PDFView](#) [Record in Scopus](#)

[Guo et al., 2009](#)

W. Guo, J.L. Mosenfelder, W.A. Goddard III, J.M. Eiler **Isotopic fractionations associated with phosphoric acid digestion of carbonate minerals: Insights from first-principles theoretical modeling and clumped isotope measurements**

Geochim. Cosmochim. Acta, 73 (2009), pp. 7203-7225

[ArticleDownload](#) [PDFView](#) [Record in Scopus](#)

[Henkes et al., 2013](#)

G.A. Henkes, B.H. Passey, A.D. Wanamaker, E.L. Grossman, W.G. Ambrose, M.L. Carroll **Carbonate clumped isotope compositions of modern marine mollusk and brachiopod shells**

Geochim. Cosmochim. Acta (2013)

[Henkes et al., 2014](#)

G.A. Henkes, B.H. Passey, E.L. Grossman, B.J. Shenton, A. Pérez-Huerta, T.E. Yancey **Temperature limits for preservation of primary calcite clumped isotope paleotemperatures**

Geochim. Cosmochim. Acta, 139 (2014), pp. 362-382

[ArticleDownload](#) [PDFView](#) [Record in Scopus](#)

[Hiatt and Budd, 2001](#)

E.E. Hiatt, D.A. Budd **Sedimentary phosphate formation in warm shallow waters: new insights into the palaeoceanography of the Permian Phosphoria Sea from analysis of phosphate oxygen isotopes**

Sed. Geol., 145 (2001), pp. 119-133

[ArticleDownload](#) [PDFView](#) [Record in Scopus](#)



[Huntington et al.](#)

K. Huntington, J. Eiler, H. Affek, W. Guo, M. Bonifacie, L. Yeung, N.Thiagarajan, B. Passey, A. Tripati, M. Daëron **Methods and limitations of 'clumped' CO<sub>2</sub> isotope ( $\Delta_{47}$ ) analysis by gas-source isotope ratio mass spectrometry**

J. Mass Spectrom., 44 (2009), pp. 1318-1329

[CrossRefView Record in Scopus](#)

[Jaffrés et al., 2007](#)

J.B.D. Jaffrés, G.A. Shields, K. Wallmann **The oxygen isotope evolution of seawater: a critical review of a long-standing controversy and an improved geological water cycle model for the past 3.4 billion years**

Earth Sci. Rev., 83 (2007), pp. 83-122

[ArticleDownload PDFView Record in Scopus](#)

[Jaisi and Blake, 2010](#)

D.P. Jaisi, R.E. Blake **Tracing sources and cycling of phosphorus in Peru Margin sediments using oxygen isotopes in authigenic and detrital phosphates**

Geochim. Cosmochim. Acta, 74 (2010), pp. 3199-3212

[ArticleDownload PDFView Record in Scopus](#)

[Jarvis, 1992](#)

I. Jarvis **Sedimentology, geochemistry and origin of phosphatic chalks: the Upper Cretaceous deposits of NW Europe**

Sedimentology, 39 (1992), pp. 55-97

[CrossRefView Record in Scopus](#)

[Karhu and Epstein, 1986](#)

J. Karhu, S. Epstein **The implication of the oxygen isotope records in coexisting cherts and phosphates**

Geochim. Cosmochim. Acta, 50 (1986), pp. 1745-1756

[ArticleDownload PDFView Record in Scopus](#)

[Kasting et al., 2006](#)

J.F. Kasting, M.T. Howard, K. Wallmann, J. Veizer, G. Shields, J. Jaffrés **Paleoclimates, ocean depth, and the oxygen isotopic composition of seawater**

Earth Planet. Sci. Lett., 252 (2006), pp. 82-93

[ArticleDownload PDFView Record in Scopus](#)

[Kastner et al., 1990](#)

M. Kastner, R. Garrison, Y. Kolodny, C. Reimers, A. Shemesh **Coupled changes of oxygen isotopes in PO<sub>4</sub><sup>3-</sup> and CO<sub>3</sub><sup>2-</sup> in apatite, with emphasis on the Monterey Formation, California**

Phosphate Deposits of the World, 3 (1990), pp. 312-324

[View Record in Scopus](#)

[Killingley, 1983](#)

J.S. Killingley **Effects of diagenetic recrystallization on <sup>18</sup>O/<sup>16</sup>O values of deep-sea sediments**

Nature, 301 (1983), pp. 594-597

[CrossRefView Record in Scopus](#)

[Kim and O'Neil, 1997](#)

S.T. Kim, J.R. O'Neil **Equilibrium and nonequilibrium oxygen isotope effects in synthetic carbonates**

Geochim. Cosmochim. Acta, 61 (1997), pp. 3461-3475

[ArticleDownload PDFView Record in Scopus](#)

[Kluge et al., 2015](#)

T. Kluge, C.M. John, A.-L. Jourdan, S. Davis, J. Crawshaw **Laboratory calibration of the calcium carbonate clumped isotope thermometer in the 25–250 °C temperature range**

Geochim. Cosmochim. Acta, 157 (2015), pp. 213-227

[ArticleDownload PDFView Record in Scopus](#)

[Knauth and Epstein, 1976](#)

L.P. Knauth, S. Epstein **Hydrogen and oxygen isotope ratios in nodular and bedded cherts**

Geochim. Cosmochim. Acta, 40 (1976), pp. 1095-1108

[ArticleDownload PDFView Record in Scopus](#)

[Koch et al., 1997](#)

P.L. Koch, N. Tuross, M.L. Fogel **The effects of sample treatment and diagenesis on the isotopic integrity of carbonate in biogenic hydroxylapatite**

J. Archaeol. Sci., 24 (1997), pp. 417-430

[View Record in Scopus](#)

[Kohn and Cerling, 2002](#)

M.J. Kohn, T.E. Cerling **Stable isotope compositions of biological apatite**

M.J. Kohn, J.M. Rakovan, J.M. Huges (Eds.), Phosphates—Geochemical, Geobiological, and Materials Importance, Mineralogical Society of America, Washington, DC (2002), pp. 455-488

[CrossRefView Record in Scopus](#)

[Kolodny and Kaplan, 1970](#)

Y. Kolodny, I. Kaplan **Carbon and oxygen isotopes in apatite CO<sub>2</sub> and co-existing calcite from sedimentary phosphorite**

J. Sediment. Res., 40 (1970), pp. 954-959

[View Record in Scopus](#)

[Kolodny and Luz, 1991](#)

Y. Kolodny, B. Luz **Oxygen isotopes in phosphates of fossil fish—Devonian to Recent**

Stable Isotope Geochem.: A Tribute to Samuel Epstein, 3 (1991), pp. 105-119

[View Record in Scopus](#)

[Kolodny et al., 1983](#)

Y. Kolodny, B. Luz, O. Navon **Oxygen isotope variations in phosphate of biogenic apatites, I. Fish bone apatite—rechecking the rules of the game**

Earth Planet. Sci. Lett., 64 (1983), pp. 398-404

[ArticleDownload PDFView Record in Scopus](#)

[Kolodny et al., 1996](#)

Y. Kolodny, B. Luz, M. Sander, W. Clemens **Dinosaur bones: Fossils or pseudomorphs? The pitfalls of physiology reconstruction from apatitic fossils**

Palaeogeogr. Palaeoclimatol. Palaeoecol., 126 (1996), pp. 161-171

[ArticleDownload PDFView Record in Scopus](#)

[Land, 1995](#)

L.S. Land **Comment on “Oxygen and carbon isotopic composition of Ordovician brachiopods: Implications for coeval seawater” by H. Qing and J. Veizer**

Geochim. Cosmochim. Acta, 59 (1995), pp. 2843-2844

[ArticleDownload PDFView Record in Scopus](#)

[Lasaga, 1989](#)

A.C. Lasaga **A new approach to isotopic modeling of the variation of atmospheric oxygen through the Phanerozoic**

Am. J. Sci (1989), pp. 289-290

[View Record in Scopus](#)

[Lawrence and Gieskes, 1981](#)

J. Lawrence, J. Gieskes **Constraints on water transport and alteration in the oceanic crust from the isotopic composition of pore water**

J. Geophys. Res.: Solid Earth (1978–2012), 86 (1981), pp. 7924-7934

[CrossRefView Record in Scopus](#)

[Lécuyer and Allemand, 1999](#)

C. Lécuyer, P. Allemand **Modelling of the oxygen isotope evolution of seawater: Implications for the climate interpretation of the  $\delta^{18}\text{O}$  of marine sediments**

Geochim. Cosmochim. Acta, 63 (1999), pp. 351-361

[ArticleDownload PDFView Record in Scopus](#)

[Lécuyer et al., 1996](#)

C. Lécuyer, P. Grandjean, C. Emig **Determination of oxygen isotope fractionation between water and phosphate from living lingulids: potential application to palaeoenvironmental studies**

Palaeogeogr. Palaeoclimatol. Palaeoecol., 126 (1996), pp. 101-108

[ArticleDownload PDFView Record in Scopus](#)

[Lécuyer et al., 1998](#)

C. Lécuyer, P. Grandjean, J.-A. Barrat, J. Nolvak, C. Emig, F. Paris, M. Robardet  **$\Delta^{18}\text{O}$  and REE contents of phosphatic brachiopods: a comparison between modern and lower Paleozoic populations**

Geochim. Cosmochim. Acta, 62 (1998), pp. 2429-2436

[ArticleDownload PDFView Record in Scopus](#)

[Lécuyer et al., 2010](#)

C. Lécuyer, V. Balter, F. Martineau, F. Fourel, A. Bernard, R. Amiot, V. Gardien, O. Otero, S. Legendre, G. Panczer **Oxygen isotope fractionation between apatite-bound carbonate and water determined from controlled experiments with synthetic apatites precipitated at 10–37° C**  
Geochim. Cosmochim. Acta, 74 (2010), pp. 2072-2081

[ArticleDownload](#) [PDFView](#) [Record in Scopus](#)

[Lécuyer et al., 2013](#)

C. Lécuyer, R. Amiot, A. Touzeau, J. Trotter **Calibration of the phosphate  $\delta^{18}\text{O}$  thermometer with carbonate-water oxygen isotope fractionation equations**  
Chem. Geol. (2013)

[Longinelli and Nuti, 1968](#)

A. Longinelli, S. Nuti **Oxygen isotopic composition of phosphorites from marine formations**  
Earth Planet. Sci. Lett., 5 (1968), pp. 13-16

[ArticleDownload](#) [PDFView](#) [Record in Scopus](#)

[Longinelli and Nuti, 1973](#)

A. Longinelli, S. Nuti **Revised phosphate-water isotopic temperature scale**  
Earth Planet. Sci. Lett., 19 (1973), pp. 373-376

[ArticleDownload](#) [PDFView](#) [Record in Scopus](#)

[Longinelli et al., 2003](#)

A. Longinelli, H. Wierzbowski, A. Di Matteo  **$\Delta^{18}\text{O}(\text{PO}_4^{3-})$  and  $\delta^{18}\text{O}(\text{CO}_3^{2-})$  from belemnite guards from Eastern Europe: Implications for palaeoceanographic reconstructions and for the preservation of pristine isotopic values**  
Earth Planet. Sci. Lett., 209 (2003), pp. 337-350

[ArticleDownload](#) [PDFView](#) [Record in Scopus](#)

[Longinelli, 1984](#)

A. Longinelli **Oxygen isotopes in mammal bone phosphate: a new tool for paleohydrological and paleoclimatological research?**  
Geochim. Cosmochim. Acta, 48 (1984), pp. 385-390

[ArticleDownload](#) [PDFView](#) [Record in Scopus](#)

[Luz et al., 1984a](#)

B. Luz, Y. Kolodny, M. Horowitz **Fractionation of oxygen isotopes between mammalian bone-phosphate and environmental drinking water**  
Geochim. Cosmochim. Acta, 48 (1984), pp. 1689-1693

[ArticleDownload](#) [PDFView](#) [Record in Scopus](#)

[Luz et al., 1984b](#)

B. Luz, Y. Kolodny, J. Kovach **Oxygen isotope variations in phosphate of biogenic apatites, III. Conodonts**  
Earth Planet. Sci. Lett., 69 (1984), pp. 255-262

[ArticleDownload](#) [PDFView](#) [Record in Scopus](#)

[McArthur and Herczeg, 1990](#)

J. McArthur, A. Herczeg **Diagenetic stability of the isotopic composition of phosphate-oxygen: palaeoenvironmental implications**

Geol. Soc. Lond. Spec. Publ., 52 (1990), pp. 119-124

[CrossRefView Record in Scopus](#)

[McArthur et al., 1980](#)

J. McArthur, M. Coleman, J. Bremner **Carbon and oxygen isotopic composition of structural carbonate in sedimentary francolite**

J. Geol. Soc., 137 (1980), pp. 669-673

[CrossRefView Record in Scopus](#)

[McArthur et al., 1986](#)

J. McArthur, R. Benmore, M. Coleman, C. Soldi, H.-W. Yeh, G. O'Brien **Stable isotopic characterisation of francolite formation**

Earth Planet. Sci. Lett., 77 (1986), pp. 20-34

[ArticleDownload PDFView Record in Scopus](#)

[McArthur et al., 1990](#)

J. McArthur, A. Sahami, M. Thirlwall, P. Hamilton, A. Osborn **Dating phosphogenesis with strontium isotopes**

Geochim. Cosmochim. Acta, 54 (1990), pp. 1343-1351

[ArticleDownload PDFView Record in Scopus](#)

[McCrea, 1950](#)

J.M. McCrea **On the isotopic chemistry of carbonates and a paleotemperature scale**

J. Chem. Phys., 18 (1950), pp. 849-857

[CrossRefView Record in Scopus](#)

[Miller et al., 1987](#)

K.G. Miller, R.G. Fairbanks, G.S. Mountain **Tertiary oxygen isotope synthesis, sea level history, and continental margin erosion**

Paleoceanography, 2 (1987), pp. 1-19

[CrossRefView Record in Scopus](#)

[Muehlenbachs, 1986](#)

K. Muehlenbachs **Alteration of the oceanic crust and the <sup>18</sup>O history of seawater**

Rev. Mineral. Geochem., 16 (1986), pp. 425-444

[View Record in Scopus](#)

[O'Neil et al., 1969](#)

O'Neil, J.R., Clayton, R.N., Mayeda, T.K., 1969. Oxygen isotope fractionation in divalent metal carbonates. Univ. Chicago.

[Passey and Henkes, 2012](#)

B. Passey, G. Henkes **Carbonate clumped isotope bond reordering and geospeedometry**

Earth Planet. Sci. Lett., 351-352 (2012), pp. 223-236

[ArticleDownload PDFView Record in Scopus](#)

[Passey et al., 2007](#)

B.H. Passey, T.E. Cerling, N.E. Levin **Temperature dependence of oxygen isotope acid fractionation for modern and fossil tooth enamels**

Rapid Commun. Mass Spectrom., 21 (2007), pp. 2853-2859

[CrossRefView Record in Scopus](#)

[Passey et al., 2010](#)

B.H. Passey, N.E. Levin, T.E. Cerling, F.H. Brown, J.M. Eiler **High-temperature environments of human evolution in East Africa based on bond ordering in paleosol carbonates**

Proc. Natl. Acad. Sci., 107 (2010), p. 11245

[CrossRefView Record in Scopus](#)

[Petersen and Schrag, 2015](#)

S. Petersen, D. Schrag **Antarctic ice growth before and after the Eocene-Oligocene transition: new estimates from clumped isotope paleothermometry**

Paleoceanography, 30 (2015), pp. 1305-1317

[CrossRefView Record in Scopus](#)

[Pucéat et al., 2010](#)

E. Pucéat, M.M. Joachimski, A. Bouilloux, F. Monna, A. Bonin, S. Motreuil, P. Morinière, S. Hénard, J. Mourin, G. Dera **Revised phosphate-water fractionation equation reassessing paleotemperatures derived from biogenic apatite**

Earth Planet. Sci. Lett., 298 (2010), pp. 135-142

[ArticleDownload PDFView Record in Scopus](#)

[Reeves and Rothman, 2013](#)

D. Reeves, D.H. Rothman **Age dependence of mineral dissolution and precipitation rates**

Global Biogeochem. Cycles, 27 (2013), pp. 906-919

[CrossRefView Record in Scopus](#)

[Sadaqah et al., 2007](#)

R.M. Sadaqah, A.M. Abed, K.A. Grimm, P.K. Pufahl **Oxygen and carbon isotopes in Jordanian phosphorites and associated fossils**

J. Asian Earth Sci., 29 (2007), pp. 803-812

[ArticleDownload PDFView Record in Scopus](#)

[Saenger et al., 2012](#)

C. Saenger, H.P. Affek, T. Felis, N. Thiagarajan, J.M. Lough, M. Holcomb **Carbonate clumped isotope variability in shallow water corals: temperature dependence and growth-related vital effects**

Geochim. Cosmochim. Acta, 99 (2012), pp. 224-242

[ArticleDownload PDFView Record in Scopus](#)

[Schauble et al., 2006](#)

E.A. Schauble, P. Ghosh, J.M. Eiler **Preferential formation of  $^{13}\text{C}$ - $^{18}\text{O}$  bonds in carbonate minerals, estimated using first-principles lattice dynamics**

Geochim. Cosmochim. Acta, 70 (2006), pp. 2510-2529

[ArticleDownload PDFView Record in Scopus](#)

[Schrag et al., 1992](#)

D.P. Schrag, D.J. DePaolo, F.M. Richter **Oxygen isotope exchange in a two-layer model of oceanic crust**

Earth Planet. Sci. Lett., 111 (1992), pp. 305-317

[ArticleDownload PDFView Record in Scopus](#)

[Schrag et al., 1995](#)

D.P. Schrag, D.J. DePaolo, F.M. Richter **Reconstructing past sea surface temperatures: correcting for diagenesis of bulk marine carbonate**

Geochim. Cosmochim. Acta, 59 (1995), pp. 2265-2278

[ArticleDownload PDFView Record in Scopus](#)

[Sharp et al., 2000](#)

Z.D. Sharp, V. Atudorei, H. Furrer **The effect of diagenesis on oxygen isotope ratios of biogenic phosphates**

Am. J. Sci., 300 (2000), pp. 222-237

[CrossRefView Record in Scopus](#)

[Shemesh et al., 1983](#)

A. Shemesh, Y. Kolodny, B. Luz **Oxygen isotope variations in phosphate of biogenic apatites, II. Phosphorite rocks**

Earth Planet. Sci. Lett., 64 (1983), pp. 405-416

[ArticleDownload PDFView Record in Scopus](#)

[Shemesh et al., 1988](#)

A. Shemesh, Y. Kolodny, B. Luz **Isotope geochemistry of oxygen and carbon in phosphate and carbonate of phosphorite francolite**

Geochim. Cosmochim. Acta, 52 (1988), pp. 2565-2572

[ArticleDownload PDFView Record in Scopus](#)

[Shemesh, 1990](#)

A. Shemesh **Crystallinity and diagenesis of sedimentary apatites**

Geochim. Cosmochim. Acta, 54 (1990), pp. 2433-2438

[ArticleDownload PDFView Record in Scopus](#)

[Silverman et al., 1952](#)

S.R. Silverman, R.K. Fuyat, J.D. Weiser **Quantitative determination of calcite associated with carbonate-bearing apatites**

Am. Mineral., 37 (1952), pp. 211-222

[View Record in Scopus](#)

[Stern et al., 1968](#)

M.J. Stern, W. Spindel, E. Monse **Temperature dependences of isotope effects**

J. Chem. Phys., 48 (1968), p. 2908

[CrossRefView Record in Scopus](#)

[Stolper and Eiler, 2015](#)

D.A. Stolper, J.M. Eiler **The kinetics of solid-state isotope-exchange reactions for clumped isotopes: a study of inorganic calcites and apatites from natural and experimental samples**  
Am. J. Sci., 315 (2015), pp. 363-411

[CrossRefView Record in Scopus](#)

[Stolper, 2014](#)

Stolper D. A. (2014) New insights into the formation and modification of carbonate-bearing minerals and methane gas in geological systems using multiply substituted isotopologues, Geological and Planetary Sciences. California Institute of Technology, p. 305.

[Sun et al., 2012](#)

Y. Sun, M.M. Joachimski, P.B. Wignall, C. Yan, Y. Chen, H. Jiang, L. Wang, X. Lai **Lethally hot temperatures during the Early Triassic greenhouse**  
Science, 338 (2012), pp. 366-370

[CrossRefView Record in Scopus](#)

[Swart et al.,  
1991](#)

P.K. Swart, S. Burns, J. Leder **Fractionation of the stable isotopes of oxygen and carbon in carbon dioxide during the reaction of calcite with phosphoric acid as a function of temperature and technique**

Chem. Geol.: Isot. Geosci. Sec., 86 (1991), pp. 89-96

[ArticleDownload PDFView Record in Scopus](#)

[Thomson et al.,  
1984](#)

J. Thomson, S. Calvert, S. Mukherjee, W. Burnett, J. Bremner **Further studies of the nature, composition and ages of contemporary phosphorite from the Namibian Shelf**

Earth Planet. Sci. Lett., 69 (1984), pp. 341-353

[ArticleDownload PDFView Record in Scopus](#)

[I  
i  
c  
h  
o  
m  
i  
r  
o  
w](#)



M. Tichomirowa, G. Grosche, J. Götze, B. Belyatsky, E. Savva, J. Keller, W. Todt **The mineral isotope composition of two Precambrian carbonatite complexes from the Kola Alkaline Province — Alteration versus primary magmatic signatures**

Lithos, 91 (2006), pp. 229-249

[ArticleDownload PDFView Record in Scopus](#)

[Trotter et al., 2008](#)

J.A. Trotter, I.S. Williams, C.R. Barnes, C. Lécuyer, R.S. Nicoll **Did cooling oceans trigger Ordovician biodiversification? Evidence from conodont thermometry**

Science, 321 (2008), pp. 550-554

[CrossRefView Record in Scopus](#)

[Tudge, 1960](#)

A. Tudge **A method of analysis of oxygen isotopes in orthophosphate—its use in the measurement of paleotemperatures**

Geochim. Cosmochim. Acta, 18 (1960), pp. 81-93

[ArticleDownload PDFView Record in Scopus](#)

[Urey et al., 1951](#)

H.C. Urey, H.A. Lowenstam, S. Epstein, C.R. McKinney **Measurement of paleotemperatures and temperatures of the Upper Cretaceous of England, Denmark, and the southeastern United States**

Geol. Soc. Am. Bull., 62 (1951), pp. 399-416

[CrossRefView Record in Scopus](#)

[Urey, 1947](#)

H.C. Urey **The thermodynamic properties of isotopic substances**

J. Chem. Soc. (1947), pp. 562-581

[CrossRefView Record in Scopus](#)

[Veizer and Prok](#)

J. Veizer, A. Prokoph **Temperatures and oxygen isotopic composition of Phanerozoic oceans**

Earth Sci. Rev., 146 (2015), pp. 92-104

[ArticleDownload PDFView Record in Scopus](#)

[Veizer et al., 198](#)

J. Veizer, P. Fritz, B. Jones **Geochemistry of brachiopods: oxygen and carbon isotopic records of Paleozoic oceans**

Geochim. Cosmochim. Acta, 50 (1986), pp. 1679-1696

[ArticleDownload PDFView Record in Scopus](#)

[Veizer et al., 199](#)

J. Veizer, P. Bruckschen, F. Pawellek, A. Diener, O.G. Podlaha, G.A. Carden, T. Jasper, C. Korte, H. Strauss, K. Azmy **Oxygen isotope evolution of Phanerozoic seawater**

Palaeogeogr. Palaeoclimatol. Palaeoecol., 132 (1997), pp. 159-172

[ArticleDownload PDFView Record in Scopus](#)

[Veizer et al., 199](#)

J. Veizer, D. Ala, K. Azmy, P. Bruckschen, D. Buhl, F. Bruhn, G.A. Carden, A. Diener, S. Ebner, Y. Godderis  **$^{87}\text{Sr}/^{86}\text{Sr}$ ,  $\delta^{13}\text{C}$  and  $\delta^{18}\text{O}$  evolution of Phanerozoic seawater**

Chem. Geol., 161 (1999), pp. 59-88

[ArticleDownload PDFView Record in Scopus](#)

[Wacker et al., 20](#)

U. Wacker, J. Fiebig, B.R. Schoene **Clumped isotope analysis of carbonates: comparison of two different acid digestion techniques**

Rapid Commun. Mass Spectrom., 27 (2013), pp. 1631-1642

[CrossRefView Record in Scopus](#)

[Wacker et al., 20](#)

U. Wacker, J. Fiebig, J. Tödter, B.R. Schöne, A. Bahr, O. Friedrich, T. Tütken, E. Gischler, M.M. Joachimski **Empirical calibration of the clumped isotope paleothermometer using calcites of various origins**

Geochim. Cosmochim. Acta, 141 (2014), pp. 127-144

[ArticleDownload PDFView Record in Scopus](#)

[Wang et al., 200](#)

Z. Wang, E.A. Schauble, J.M. Eiler **Equilibrium thermodynamics of multiply substituted isotopologues of molecular gases**

Geochim. Cosmochim. Acta, 68 (2004), pp. 4779-4797

[ArticleDownload PDFView Record in Scopus](#)

[Wenzel et al., 20](#)

B. Wenzel, C. Lécuyer, M.M. Joachimski **Comparing oxygen isotope records of silurian calcite and phosphate— $\delta^{18}\text{O}$  compositions of brachiopods and conodonts**

Geochim. Cosmochim. Acta, 64 (2000), pp. 1859-1872

[ArticleDownload](#) [PDFView](#) [Record in Scopus](#)

[Zaarur et al., 2013](#)

S. Zaarur, H.P. Affek, M.T. Brandon **A revised calibration of the clumped isotope thermometer**

Earth Planet. Sci. Lett., 382 (2013), pp. 47-57

[ArticleDownload](#) [PDFView](#) [Record in Scopus](#)

[Zazzo et al., 2004](#)

A. Zazzo, C. Lécuyer, A. Mariotti **Experimentally-controlled carbon and oxygen isotope exchange between bioapatites and water under inorganic and microbially-mediated conditions**

Geochim. Cosmochim. Acta, 68 (2004), pp. 1-12

[ArticleDownload](#) [PDFView](#) [Record in Scopus](#)

[Zhang, 1994](#)

Y. Zhang **Reaction kinetics, geospeedometry, and relaxation theory**

Earth Planet. Sci. Lett., 122 (1994), pp. 373-391

[CrossRefView](#) [Record in Scopus](#)

1

Present address: Department of Geosciences, Princeton University, Princeton, NJ 08544, United States.

2

$\delta = (R_{\text{sample}}/R_{\text{standard}} - 1) \times 1000$  where  $R = [^{13}\text{C}]/[^{12}\text{C}]$  for carbon isotopes and  $[^{18}\text{O}]/[^{16}\text{O}]$  for oxygen isotopes. For carbon isotopes, samples are referenced to the VPDB scale and for oxygen isotopes, to VSMOW.

3

$\Delta_{47} = ([^{47}\text{R}]/[^{47}\text{R}^*] - 1) \times 1000$  where  $^{47}\text{R} = [^{13}\text{C}^{16}\text{O}^{18}\text{O} + ^{12}\text{C}^{17}\text{O}^{18}\text{O} + ^{13}\text{C}^{17}\text{O}_2]/[^{12}\text{C}^{16}\text{O}_2]$  and \* denotes the random distribution.